

# Synlett

## Sulfonated Tetraphenylethylene-Based Hypercrosslinked Polymer as a Heterogeneous Catalyst for the Synthesis of Symmetrical Triarylmethanes via a Dual C–C Bond Cleaving Path

Gitumoni Kalita, Namrata Deka, Dipankar Paul, Loknath Thapa, Gitish K Dutta, Paresh N Chatterjee.

Affiliations below.

DOI: 10.1055/a-1277-3995

Please cite this article as: Kalita G, Deka N, Paul D et al. Sulfonated Tetraphenylethylene-Based Hypercrosslinked Polymer as a Heterogeneous Catalyst for the Synthesis of Symmetrical Triarylmethanes via a Dual C–C Bond Cleaving Path. Synlett 2020. doi: 10.1055/a-1277-3995

**Conflict of Interest:** The authors declare that they have no conflict of interest.

**This study was supported by** Science and Engineering Research Board (<http://dx.doi.org/10.13039/501100001843>), SB/FT/CS-075/2014, SB/FT/CS-115/2014

### Abstract:

A sulfonic acid functionalized tetraphenylethylene-based hypercrosslinked polymer (THP-SO<sub>3</sub>H) with a well-developed porous network and accessible sulfonic acid sites was synthesized and characterized by different analytical techniques. The catalytic prowess of the synthesized material THP-SO<sub>3</sub>H was investigated in a challenging dual C–C bond-breaking reaction for the synthesis of symmetrical triarylmethanes (TRAMs) in high yield. The scope of the developed metal-free method was also explored with a wide variety of substrates. The organocatalyst can be easily recovered by filtration and reused up to five consecutive cycles without substantial loss in its catalytic efficacy.

### Corresponding Author:

Paresh N Chatterjee, National Institute of Technology Meghalaya, Chemistry, Bijni Complex, 793003 Shillong, India, paresh.chatterjee@nitm.ac.in

### Affiliations:

Gitumoni Kalita, National Institute of Technology Meghalaya, Chemistry, Shillong, India

Namrata Deka, National Institute of Technology Meghalaya, Chemistry, Shillong, India

Dipankar Paul, National Institute of Technology Meghalaya, Chemistry, Shillong, India

[...]

Paresh N Chatterjee, National Institute of Technology Meghalaya, Chemistry, Shillong, India

# Sulfonated Tetraphenylethylene-Based Hypercrosslinked Polymer as a Heterogeneous Catalyst for the Synthesis of Symmetrical Triarylmethanes via a Dual C–C Bond Cleaving Path

Gitumoni Kalita†  
 Namrata Deka†  
 Dipankar Paul†  
 Loknath Thapa  
 Gitish K. Dutta\*  
 Paresh Nath Chatterjee\*

Department of Chemistry, National Institute of Technology  
 Meghalaya, Bijnai Complex, Laitumkhrah, Shillong 793003,  
 Meghalaya, INDIA

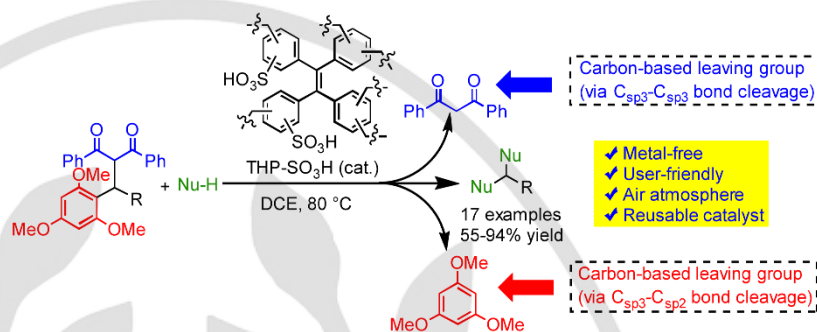
† Equal contribution

\* indicates the main/corresponding author.

paresh.chatterjee@nitm.ac.in

gitish.dutta@nitm.ac.in

Click here to insert a dedication.



Received:  
 Accepted:  
 Published online:  
 DOI:

**Abstract** A sulfonic acid functionalized tetraphenylethylene-based hypercrosslinked polymer (THP-SO<sub>3</sub>H) with a well-developed porous network and accessible sulfonic acid sites was synthesized and characterized by different analytical techniques. The catalytic prowess of the synthesized material THP-SO<sub>3</sub>H was investigated in a challenging dual C–C bond-breaking reaction for the synthesis of symmetrical triarylmethanes (TRAMs) in high yield. The scope of the developed metal-free method was also explored with a wide variety of substrates. The organocatalyst can be easily recovered by filtration and reused up to five consecutive cycles without substantial loss in its catalytic efficacy.

**Keywords** hypercrosslinked polymer, heterogeneous catalyst, reusable, C–C bond-breaking, triarylmethane.

Functionalization of porous organic polymers has provided an exciting platform for catering to a varied array of applications such as adsorption, energy applications, catalysis, etc.<sup>1</sup> The high thermal and chemical stability, high specific surface areas and hierarchical pore networks of porous organic polymers have attracted significant attention over recent decades.<sup>2</sup> Moreover, they have an added advantage of the ease of preparation and functionalization using mild synthetic conditions. The proper selection of monomer units further aids in designing polymer materials with tailor-made properties for different applications. Based on the reactions involved in the synthetic process, porous organic polymers may be further classified into the categories such as hypercrosslinked polymers, microporous organic polymers, covalent organic framework, etc.<sup>3</sup> Hypercrosslinked polymers possessing high surface areas, inherent porosity, good chemical and thermal stability and a rigid skeleton for easy incorporation of catalytic sites have been proven to be a promising candidate for their use as heterogeneous catalysts.<sup>4</sup> Heterogeneous catalysts are being gradually preferred over classical homogeneous catalysts owing to their non-corrosiveness, ease of recovery and reusability.<sup>5</sup> However, common limitations of heterogeneous catalysts include high cost, low yields and catalyst poisoning in a

hydrophilic environment. In this regard, the effective design of hypercrosslinked polymer-based catalysts may help to combine the advantages of both heterogeneous and homogeneous catalysts. Acid-functionalized hypercrosslinked polymers have been recently utilized as heterogeneous catalysts, mostly for the conversion of biomass to biofuel,<sup>6</sup> biofuel additives<sup>7</sup> and hydroxymethylfurfural (HMF).<sup>8</sup> Bhaumik and his group have recently employed a hypercrosslinked supermicroporous polymer as a heterogeneous catalyst for synthesizing biodiesel.<sup>6</sup> However, the scope of such functionalized polymer-based catalysts has not been investigated much in other organic synthetic applications.

For example, organic reactions proceeding through unusual yet challenging C–C bond-breaking reactions still await the same level of interest as C–C bond-forming counterparts. Over the past years, several catalytic routes for the cleavage of the C–C bonds have been developed by researchers.<sup>11</sup> Our interest on exploring new catalytic approaches for the activation of C–C bonds, lead us to develop a facile FeCl<sub>3</sub> catalyzed dual C–C bond-breaking reaction in homogeneous medium for the synthesis of symmetrical and unsymmetrical triarylmethanes (TRAMs).<sup>12</sup> In spite of tremendous reactivity and selectivity of homogeneous catalysts, it has limited applications in industrial processes due to the difficulties associated with the removal, recovery, and recycling of the active catalysts. Till date, several methods are reported in the literature on the synthesis of TRAMs.<sup>13</sup> To the best of our knowledge, the synthesis of TRAMs via a dual C–C bond-breaking reaction of diarylmethyl substituted 1,3-dicarbonyl derivatives **1** has not been attempted with heterogeneous catalysts. In this regard, acid-functionalized hypercrosslinked polymers can be used as reusable heterogeneous catalyst for the synthesis of TRAMs. Here, we have synthesized a sulfonic acid functionalized hypercrosslinked polymer derived from tetraphenylethylene (TPE). Hypercrosslinked polymers have been previously used by researchers as polymeric supports due to their porous natures and high thermal stabilities.<sup>14</sup> However, the choice of monomer units heavily influences the physico-chemical

characteristics of the polymer. The tetraphenylethylene (TPE) moiety consists of peripheral phenyl rings, which prevents the  $\pi$ - $\pi$  stacking of its polymerized form. Hence, the surface area of TPE-based hypercrosslinked polymers is usually very high and provides a suitable platform for the incorporation of numerous catalytic sites. Moreover, increasing the crosslinking between the monomer units improves the thermal stability of the polymeric catalyst. The synthesized TPE-based hypercrosslinked polymer (THP) has a high surface area and optimum pore dimensions, which make it a suitable framework for introducing sulfonic acid sites. The sulfonated polymer (THP-SO<sub>3</sub>H) possesses high sulfonic acid content and good thermal stability. Also, THP-SO<sub>3</sub>H shows high potential as a heterogeneous catalyst for the synthesis of symmetrical TRAMs via a dual C–C bond-breaking reaction of diarylmethyl substituted 1,3-dicarbonyl derivatives **1**. It is noteworthy to mention that, TRAM skeleton is found in several natural products, pharmaceuticals, dyes etc.<sup>15</sup> Moreover, the application of THP-SO<sub>3</sub>H as a reusable heterogeneous catalyst in the dual C–C bond-breaking reaction enhances the practical utility of the present work.

The tetraphenylethylene-based hypercrosslinked polymer (THP) scaffold was synthesized via a simple Friedel–Crafts based crosslinking reaction with tetraphenylethylene as the monomer and formaldehyde dimethylacetal as the crosslinker.<sup>16</sup> Sulfonation of the polymer was successfully carried out in chlorosulfonic acid (ClSO<sub>3</sub>H) at 25 °C under N<sub>2</sub> atmosphere (Scheme S1 of ESI).<sup>6</sup> The details of the structural and morphological characterizations of THP-SO<sub>3</sub>H are included in the ESI.

After characterizing the THP-SO<sub>3</sub>H material, we were interested to explore its catalytic prowess for the synthesis of symmetrical TRAMs via a challenging dual C–C bond-cleaving reaction of diarylmethyl substituted 1,3-dicarbonyl derivatives **1** in a heterogeneous medium. To investigate the optimized reaction conditions, we chose 1,3-diphenyl-2-(phenyl(2,4,6-trimethoxyphenyl)methyl)propane-1,3-dione (**1a**) and 2-methylfuran (**2a**) as the model substrates for the synthesis of symmetrical TRAM **3a** by the cleavage of both C<sub>sp3</sub>–C<sub>sp3</sub> and C<sub>sp3</sub>–C<sub>sp2</sub> bonds in substrate **1a** (Table 1). Initially, we screened different solvents (Table 1, entries 1–5) for the dual C–C bond cleavage in the presence of THP-SO<sub>3</sub>H to find out the suitable solvent for the reaction. Among different solvents, the highest yield of the symmetrical TRAM **3a** was obtained in DCE solvent using the synthesized organocatalyst at 80 °C in 30 min (Table 1, entry 3). The reaction gave comparably lower yield of the desired TRAM **3a** in MeNO<sub>2</sub>, MeCN and toluene solvents (Table 1, entries 1–2, 4). However, polar protic solvent, such as EtOH gave poor yield of **3a** even after 3 h (Table 1, entry 5). The temperature also played a significant role in the dual C–C bond-breaking reaction. When we decreased the temperature from 80 °C to 55 °C, only 78% yield of desired product **3a** was obtained after 3 h (Table 1, entry 6). Further decreasing the temperature to room temperature, product **3a** was obtained only in 52% yield after 5 h (Table 1, entry 7). Unlike our previous report,<sup>12</sup> we did not isolate any unsymmetrical TRAM via the cleavage of C<sub>sp3</sub>–C<sub>sp3</sub> bond only,<sup>17</sup> resulting dibenzoylmethane as the carbon-based leaving group. In addition, we varied the catalyst loading to determine the optimum amount of THP-SO<sub>3</sub>H for the dual C–C

bond cleavage in the reaction. It is noteworthy that the use of 96 mg catalyst at 80 °C produced the maximum yield of the product **3a** in 30 min (Table 1, entry 3). An increase in the amount of catalyst loading (144 mg) did not affect the yield of the reaction significantly (Table 1, entry 8). But a lower catalyst loading (48 mg) resulted in the lesser yield of the product **3a** (Table 1, entry 9). Besides, no dual C–C bond-breaking reaction was noticed in the absence of catalyst and the starting materials were recovered quantitatively (Table 1, entry 10). It is to be noted that the leaving 1,3-diphenylpropan-1,3-dione and 1,3,5-trimethoxybenzene were isolated in more than 90% yields (Table 1, entry 3).

**Table 1:** Optimization of reaction conditions<sup>a</sup>

Entry	Solvent	Temp. (°C)	Time (min)	Yield (%) <sup>b</sup>
1	MeNO <sub>2</sub>	80	45	89
2	MeCN	80	60	81
3	DCE	80	30	94
4	toluene	80	90	64
5	EtOH	80	180	56
6	DCE	55	180	78
7	DCE	RT	300	52
8 <sup>c</sup>	DCE	80	30	96
9 <sup>d</sup>	DCE	80	30	78
10 <sup>e</sup>	DCE	80	60	nil

<sup>a</sup>Reaction conditions: **1a** (480 mg, 1.0 mmol), **2a** (246 mg, 3.0 mmol), catalyst (96 mg), solvent (2 mL); <sup>b</sup> Isolated yields; <sup>c</sup> catalyst (144 mg); <sup>d</sup> catalyst (48 mg); <sup>e</sup> No catalyst.

After optimizing the reaction conditions, we explored the substrate scope of the developed method with our in-house synthesized organocatalyst THP-SO<sub>3</sub>H. From our previous work, we experienced that the combination of 1,3-diphenylpropan-1,3-dione (as the 1,3-dicarbonyl substituent) and 2,4,6-trimethoxyphenyl unit (as the electron-rich arene substituent) in the starting substrates **1** showed the best results during dual C–C bond-breaking reaction.<sup>12</sup>

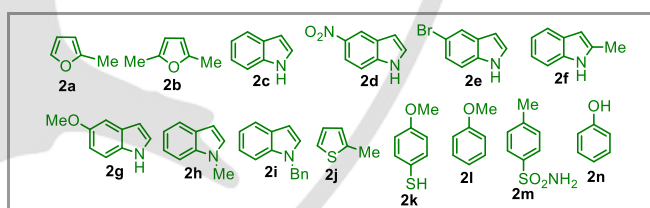
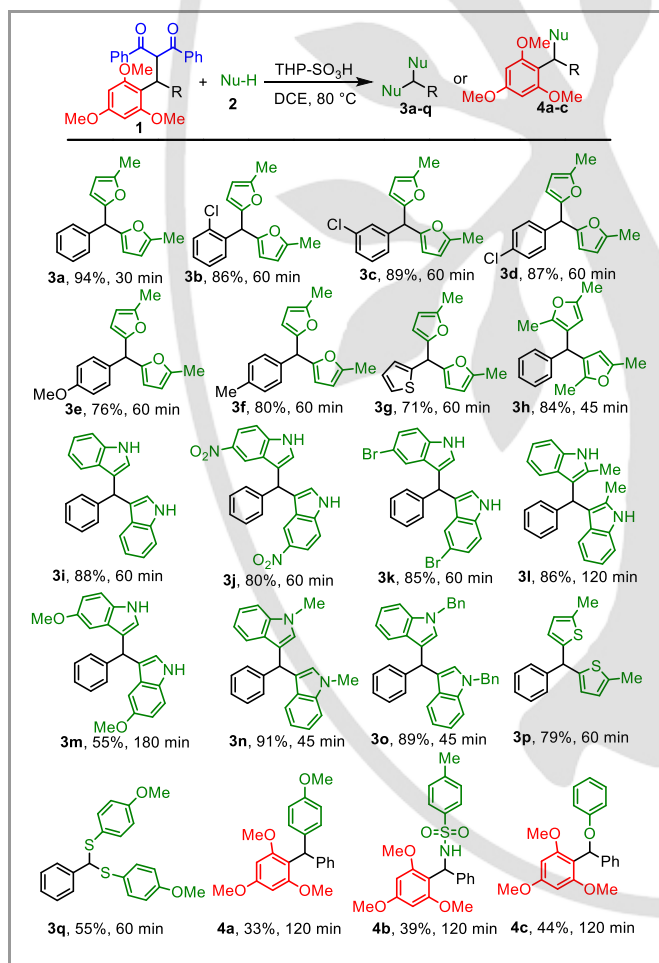


**Figure 1:** List of nucleophiles used in the dual C–C bond cleavage reaction.

Hence, to study the catalytic efficacy of THP-SO<sub>3</sub>H for the synthesis of symmetrical TRAMs, we varied only the R-group in **1**, keeping 1,3-diphenylpropan-1,3-dione and 2,4,6-trimethoxyphenyl units intact in the precursor **1** (Scheme 1). We found that the aromatic ring bearing EWG, in substrate **1** generated slightly higher yields of the symmetrical TRAMs **3b–d** than the aromatic ring bearing EDG **3e–f**. A heteroaryl substituent in substrate **1g** provided the corresponding product **3g** in 71% yield. Furthermore, the reaction performed well when 2,5-dimethylfuran (**2b**) was used as nucleophile

producing the desired TRAM **3h** in good yield. Then, we examined other nucleophiles based on their performance in dual C–C bond-cleaving reaction. In the presence of indole derivatives (**2c-i**), the corresponding bis-indolylmethanes (**3i-o**) were obtained in good yield. Surprisingly, 5-methoxyindole (**2g**) gave a lower yield of the desired bis-indolylmethane derivative **3m** after prolonged reaction time. The *N*-substituted indoles **2h-i** were effective in the dual C–C bond-cleaving reaction generating the symmetrical TRAMs **3n-o** in excellent yields. 2-Methylthiophene (**2j**) also reacted well with substrate **1a** to give the symmetrical TRAM **3p** in 79% yield. It is important to note that 4-methoxythiophenol (**2k**) took part in the reaction producing 55% yield of the product **3q** with two new C<sub>sp3</sub>–S bonds at the cost of two C–C bonds. While examining the scope of nucleophiles, we noticed that the symmetrical TRAM did not form during the reactions between substrate **1a** and nucleophiles **2l-n** via the dual C–C bond-breaking reaction. Instead, we isolated unsymmetrical TRAMs **4** due to the exclusive C<sub>sp3</sub>–C<sub>sp3</sub> bond-cleaving reaction of **1a** in the presence of the above mentioned nucleophiles. We previously noted the similar observations in our FeCl<sub>3</sub> catalyzed dual C–C bond-breaking work.<sup>12</sup> These results indicate that the C<sub>sp3</sub>–C<sub>sp3</sub> bond is relatively easier to cleave than C<sub>sp3</sub>–C<sub>sp2</sub> bond in substrate **1** under our developed reaction conditions.<sup>18</sup>



**Scheme 1:** Substrate scope of the C–C bond-breaking reaction for the synthesis of TRAMs. Reaction conditions for **3a-h**: **1** (1.0 mmol), **2a** (3.0 mmol), THP-SO<sub>3</sub>H (96 mg), DCE (2 mL), temperature 80 °C. Reaction conditions for **3i-q** and **4a-c**: **1** (1.0 mmol), **2** (2.0 mmol), THP-SO<sub>3</sub>H (96 mg), DCE (2 mL), temperature 80 °C.

In view of commercial applications, we also explored the potential for reusability of the synthesized organocatalyst THP-SO<sub>3</sub>H in the dual C–C bond-breaking reaction of substrate **1a** and **2a**. After 30 min of the reaction time in each cycle, the catalyst was recovered by filtration, washed with DCE and dried at 100 °C under vacuum oven for 3 h (the detailed procedure is given in ESI). The recovered catalyst was reused for four consecutive cycles without significant loss in its catalytic efficiency (Figure 2).

The FT-IR spectrum of the reused catalyst after the fifth cycle shows the same pattern as the synthesized THP-SO<sub>3</sub>H material (Figure S7 of ESI), which indicates that the active site of the heterogeneous catalyst remains intact even after the fifth cycle.

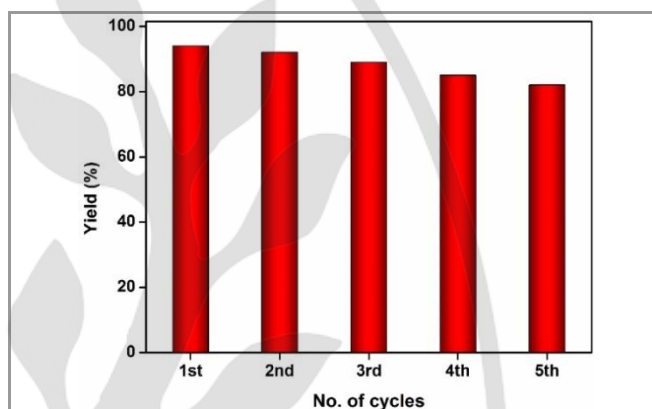
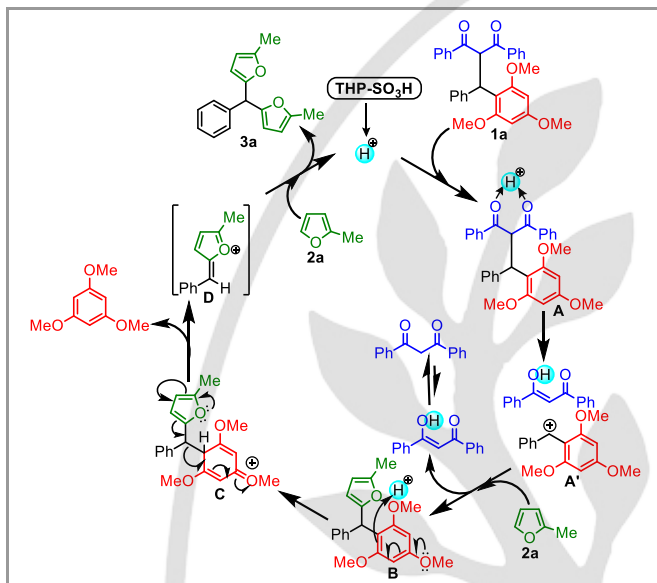


**Figure 2:** Recyclability of THP-SO<sub>3</sub>H catalyst in the dual C–C bond-breaking reaction.

Based on the above observations and the related literature about the dual C–C bond-breaking reaction, we propose a plausible reaction mechanism for the reaction between substrate **1a** and **2a** in the scheme 2. THP-SO<sub>3</sub>H has abundant acidic sites due to the presence of a large number of -SO<sub>3</sub>H groups at the surface of the hypercrosslinked polymer and provides ample H<sup>+</sup> ion in the reaction medium. The reaction may be initiated by the activation of carbonyl groups of the starting material **1a** in the presence of H<sup>+</sup> to produce a species **A**.<sup>12</sup> 2-Methylfuran (**2a**) combines with the electrophilic species **A** to form unsymmetrical TRAM **B** and consequently releases 1,3-diphenylpropan-1,3-dione by the cleavage of C<sub>sp3</sub>–C<sub>sp3</sub> bond. The electron-donating -OMe group of the species **B** undergoes conjugation and gets protonated in the acidic medium to generate an ionic species **C** which may decompose to species **D** via the elimination of 1,3,5-trimethoxybenzene.<sup>19</sup> Subsequently, a second molecule of **2a** reacts with the electrophilic center in species **D** to produce the desired symmetrical TRAM **3a** via a C<sub>sp3</sub>–C<sub>sp2</sub> bond-breaking reaction and a proton is consequently released in the reaction medium.

In conclusion, we have synthesized a novel sulfonic acid functionalized tetraphenylethylene-based hypercrosslinked polymer (THP-SO<sub>3</sub>H) with a porous network and accessible sulfonic acid sites. Due to the abundant accessible acidic sites in the material, its catalytic property was examined on a dual C–C bond-breaking reaction in diarylmethyl substituted 1,3-dicarbonyl derivatives. THP-SO<sub>3</sub>H showed promising catalytic activity in the synthesis of symmetrical TRAMs via the cleavage of both C<sub>sp3</sub>–C<sub>sp3</sub> and C<sub>sp3</sub>–C<sub>sp2</sub> bonds in mild reaction conditions.<sup>20</sup> The generality of the reaction was explored on a

diverse range of substrates and the desired product was obtained in high yield. Due to its heterogeneity in the reaction medium, the catalyst could be recycled for further use. The catalyst was reused up to five reaction cycles without any substantial decrease in its catalytic efficiency. The results described here demonstrate the first-ever synthesis of symmetrical TRAMs via a metal-free, dual C–C bond-breaking strategy using sulfonated tetraphenylethylene-based hypercrosslinked polymer as a heterogeneous catalyst.



**Scheme 2:** Plausible reaction mechanism for the reaction between **1a** and **2a** catalyzed by THP-SO<sub>3</sub>H.

### Funding Information

SERB is gratefully acknowledged for financial support to G. K. D. (grant no. SB/FT/CS-075/2014) and P. N. C. (grant no. SB/FT/CS-115/2014).

### Acknowledgment

We thank NIT Meghalaya for financial support to G. K., N. D. and D. P. SAIF, NEHU; NMR Research Centre, IISc Bangalore; SAIC, TU; Centre for Energy, IIT Guwahati; MSE, IIT Kanpur and SAIF, IIT Bombay are also acknowledged for analytical facilities.

### Supporting Information

YES (this text will be updated with links prior to publication)

### References and Notes

- (1) (a) Guillerm, V.; Weseliński, Ł. J.; Alkordi, M.; Mohideen, M. I. H.; Belmabkhout, Y.; Cairns, A. J.; Eddaoudi, M. *Chem. Commun.* **2014**, 50, 1937. (b) Hao, S.; Liu, Y.; Shang, C.; Liang, Z.; Yu, J. *Polym. Chem.* **2017**, 8, 1833. (c) Dawson, R.; Cooper, A. I.; Adams, D. J. *Polym. Int.* **2013**, 62, 345.
- (2) Zhang, Y.; Riduan, S. N. *Chem. Soc. Rev.* **2012**, 41, 2083.
- (3) Ahmed, D. S.; El-Hiti, G. A.; Yousif, E.; Ali, A. A.; Hameed, A. S. *J. Polym. Res.* **2018**, 25, 75.
- (4) Huang, J.; Turner, S. R. *Polym. Rev.* **2018**, 58, 1.

- (5) Davies, I. W.; Matty, L.; Hughes, D. L.; Reider, P. J. *J. Am. Chem. Soc.* **2001**, 123, 10139.
- (6) Bhunia, S.; Banerjee, B.; Bhaumik, A. *Chem. Commun.* **2015**, 51, 5020.
- (7) Kundu, S. K.; Singuru, R.; Hayashi, T.; Hijikata, Y.; Irle, S.; Mondal, J. *ChemistrySelect* **2017**, 2, 4705.
- (8) Du, M.; Agrawal, A. M.; Chakraborty, S.; Garibay, S. J.; Limvorapitux, R.; Choi, B.; Madrahimov, S. T.; Nguyen, S. T. *ACS Sustain. Chem. Eng.* **2019**, 7, 8126.
- (11) (a) Yao, X.; Li, C. J. *J. Org. Chem.* **2005**, 70, 5752. (b) Li, H.; Li, W.; Liu, W.; He, Z.; Li, Z. *Angew. Chem. Int. Ed.* **2011**, 50, 2975. (c) Mahoney, S. J.; Lou, T.; Bondarenko, G.; Fillion, E. *Org. Lett.* **2012**, 14, 3474. (d) Armstrong, E. L.; Grover, H. K.; Kerr, M. A. *J. Org. Chem.* **2013**, 78, 10534. (e) Yang, Y.; Ni, F.; Shu, W. M.; Wu, A. X. *Chem. Eur. J.* **2014**, 20, 11776. (f) Yao, Q.; Kong, L.; Wang, M.; Yuan, Y.; Sun, R.; Li, Y. *Org. Lett.* **2018**, 20, 1744. (g) Yao, Q.; Kong, L.; Zhang, F.; Tao, X.; Li, Y. *Adv. Synth. Catal.* **2017**, 359, 3079. (h) Cheng, X.; Zhou, Y.; Zhnag, F.; Zhu, K.; Liu, Y.; Li, Y. *Chem. Eur. J.* **2016**, 22, 12655. (i) Zhou, Y.; Tao, X.; Yao, Q.; Zhao, Y.; Li, Y. *Chem. Eur. J.* **2016**, 22, 17936.
- (12) Paul, D.; Khatua, S.; Chatterjee, P. N. *New J. Chem.* **2019**, 43, 10056.
- (13) (a) Esquivias, J.; Gomez Arrayas, R.; Carretero, J. C. *Angew. Chem. Int. Ed.* **2006**, 45, 629. (b) Mondal, S.; Panda, G. *RSC Adv.* **2014**, 4, 28317. (c) Yue, C.; Na, F.; Fang, X.; Cao, Y.; Antilla, J. C. *Angew. Chem. Int. Ed.* **2018**, 57, 11004. (d) Zhang, X.; Wang, H.; Qiu, N.; Kong, Y.; Zeng, W.; Zhang, Y.; Zhao, J. *J. Org. Chem.* **2018**, 83, 8710.
- (14) Lee, J. -S. M.; Briggs, M. E.; Hasell, T.; Copper, A. I. *Adv. Mater.* **2016**, 28, 9804.
- (15) (a) Nambo, M.; Crudden, C. M. *ACS Catal.* **2015**, 5, 4734. (b) Praveen, P. J.; Parameswaran, P. S.; Majik, M. S. *Synthesis* **2015**, 47, 1827. (c) Shiri, M.; Zolfigol, M. A.; Kruger, H. G.; Tanbakouchian, Z. *Chem. Rev.* **2010**, 110, 2250.
- (16) Zeng, J. H.; Wang, Y. F.; Gou, S. Q.; Zhang, L. P.; Chen, Y.; Jiang, J. X.; Shi, F. *ACS Appl. Mater. Interfaces* **2017**, 9, 34783.
- (17) The following unsymmetrical TRAM (via only C<sub>sp3</sub>-C<sub>sp3</sub> bond cleavage) was not isolated in the reaction.



- (18) Luo, Y. -R.; Kerr, J. *CRC Handbook of Chemistry and Physics* **2012**, 89, 89.
- (19) (a) Thirupathi, P.; Soo Kim, S. *J. Org. Chem.* **2010**, 75, 5240. (b) Castellani, C. B.; Perotti, A.; Scriveranti, M.; Vidari, G. *Tetrahedron* **2000**, 56, 8161.
- (20) **Typical procedure for the synthesis of 3a**  
A 25 mL round-bottom flask equipped with a magnetic bar and water condenser were charged with **1a** (1.0 mmol), **2a** (3.0 mmol), DCE (2.0 mL) and THP-SO<sub>3</sub>H (96 mg) in an air atmosphere. The flask was placed in a constant temperature oil-bath at 80 °C and the progress of the reaction was monitored by TLC. After 30 min, the mixture was filtered to separate the catalyst and washed twice with DCE (2 x 5 mL). Then the filtrate was removed under reduced pressure and the crude product was purified by dry column vacuum chromatography (silica gel, petroleum ether 60-80 °C/EtOAc) to give a yellow oily liquid; yield: 94%.  
<sup>1</sup>H NMR (400 MHz, CDCl<sub>3</sub>): δ (ppm) 2.158 (s, 6H), 5.256 (s, 1H), 5.788 (d, J = 3.2 Hz, 4H), 7.159–7.243 (m, 5H). <sup>13</sup>C NMR (100 MHz, CDCl<sub>3</sub>): δ (ppm) 13.65, 45.12, 106.08, 108.19, 126.97, 128.40, 128.44, 140.00, 151.46, 152.85.

**Sulfonated Tetraphenylethylene-Based Hypercrosslinked Polymer as a Heterogeneous Catalyst for the Synthesis of Symmetrical Triarylmethanes via a Dual C–C Bond Cleaving Path**

Gitumoni Kalita,† Namrata Deka,† Dipankar Paul,† Loknath Thapa, Gitish K. Dutta,\* Paresh Nath Chatterjee\*

Department of Chemistry, National Institute of Technology Meghalaya, Bijni Complex, Laitumkhrah, Shillong 793003, Meghalaya, INDIA

† Equal contribution

\* Corresponding author

Email of corresponding authors: paresh.chatterjee@nitm.ac.in

gitish.dutta@nitm.ac.in

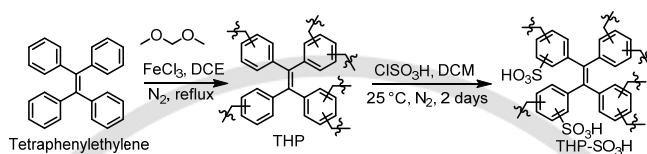
**Supplementary Material**

	<b>Contents</b>	<b>Page</b>
1	General remarks	2
2	Synthesis of sulfonated THP (THP-SO <sub>3</sub> H)	3
3	Characterization of THP-SO <sub>3</sub> H material	3-6
4	Calculation of acid strength of THP-SO <sub>3</sub> H material	7
5	General procedure for the optimization of reaction conditions	7-8
6	General procedure for the synthesis of TRAMs <b>3a-g</b>	8
7	General procedure for the synthesis of TRAMs <b>3h-q</b> and <b>4</b>	8
8	General procedure for recyclability of the catalyst THP-SO <sub>3</sub> H	8
9	FT-IR spectra of THP-SO <sub>3</sub> H material after the fifth cycle	9
10	Analytical data of products <b>3</b> and <b>4</b>	9-14
11	References	15
12	<sup>1</sup> H and <sup>13</sup> C NMR spectra of products <b>3</b> and <b>4</b>	16-35

## 1. General remarks

All reagents and solvents are of analytical reagent (AR) grade and were procured from SRL, Spectrochem, Merck, and Alfa Aesar. Solvents were distilled prior to use. All the reactions were done in oven-dried glass apparatus in an air atmosphere unless otherwise mentioned. Progress of the reactions was monitored by TLC on silica gel 60 F<sub>254</sub> using UV light and *p*-anisaldehyde stain as visualizing agents. All the organic products were purified by dry column vacuum chromatography using silica gel G as the stationary phase and petroleum ether 60-80 °C/ethyl acetate as the eluent. <sup>1</sup>H and <sup>13</sup>C NMR spectra of synthesized TRAMs were measured on a BrukerAvance II (<sup>1</sup>H NMR: 400 MHz and <sup>13</sup>C NMR: 100 MHz) spectrometer. Chemical shifts are reported in ppm from TMS, with the solvent resonance as the internal standard (unless otherwise mentioned, chloroform:  $\delta$  7.26 ppm). Data are reported as follows: chemical shifts, multiplicity (s=singlet, d=doublet, t=triplet, q=quartet, br=broad, dd=double doublet, m=multiplet), coupling constant (in Hz), integration. <sup>13</sup>C NMR spectra were recorded at 100 MHz with proton decoupling. Chemical shifts are reported in ppm from TMS with the solvent resonance as the internal standard (unless otherwise mentioned, chloroform:  $\delta$  77.0 ppm). Elemental analyses were carried out using a FlashEA 1112 elemental analyzer. Fourier transform infrared (FT-IR) spectra of THP and THP-SO<sub>3</sub>H were recorded using PerkinElmer Spectrum Two spectrometer. The surface areas of the polymers were calculated from nitrogen adsorption-desorption isotherms measured using QuantachromeAutosorbIQ. The pore-size distributions were calculated based on NLDFT calculations using a trial version of SAIEUS software. Thermogravimetric analyses (TGA) were conducted in an inert atmosphere at a heating rate of 10 °C min<sup>-1</sup>. The solid-state <sup>13</sup>C NMR spectrum of THP-SO<sub>3</sub>H was obtained on a 400 MHz JEOL ECX400. Field emission scanning electron microscopy (FESEM) analysis was done with NOVA NANOSEM 450 instrument to analyze the surface morphologies. Tetraphenylethylene-based hypercrosslinked polymer (THP) was synthesized by following a previously reported procedure in the literature.<sup>1</sup> The various precursors **1** for the synthesis of TRAMs were also prepared by following a previously reported procedure.<sup>2-3</sup>

## 2. Synthesis of sulfonated THP (THP-SO<sub>3</sub>H)



**Scheme S1:** Synthesis of sulfonic acid functionalized tetraphenylethylene-based hypercrosslinked polymer (THP-SO<sub>3</sub>H).

Vacuum-dried THP (500 mg) was taken in a two-necked round-bottom flask with 15 mL of degassed anhydrous DCM under N<sub>2</sub> atmosphere. After the mixture was cooled to 0 °C in an ice bath, 12 mL of chlorosulfonic acid (ClSO<sub>3</sub>H) was added drop-wise from a dropping funnel with constant stirring. The mixture was further stirred at 25 °C for 2 days under N<sub>2</sub> atmosphere. The reaction mixture was quenched with ice, and the precipitate was filtered. The obtained precipitate was washed several times with double distilled water and acetone. Finally the product THP-SO<sub>3</sub>H was vacuum dried at 80 °C for 24 h.

## 3. Characterization of THP-SO<sub>3</sub>H material

The structure and morphology of the sulfonated hypercrosslinked polymer (THP-SO<sub>3</sub>H) were characterized using different analytical techniques. The amount of sulfonic acid (-SO<sub>3</sub>H) sites present in the material was quantitatively analyzed by a back-titration method. THP-SO<sub>3</sub>H material was found to contain 11.11 mmol/g acidity. The facile preparation and high scalability of the sulfonated polymer stress on the viability of the material for practical applications. FT-IR and solid-state <sup>13</sup>C NMR spectra (Figure S1 & S2) confirm the formation of the polymeric framework of THP-SO<sub>3</sub>H. The band at ~620 cm<sup>-1</sup> may be assigned to the stretching vibration of C-S bond present in the material<sup>4</sup> and thus confirms the successful anchoring of the -SO<sub>3</sub>H group to the hypercrosslinked polymer (Figure S1). The bands at ~1050 cm<sup>-1</sup> and ~1180 cm<sup>-1</sup> are due to the O=S=O group.<sup>5</sup> The band at ~2960 cm<sup>-1</sup> is attributed to the presence of unsaturated C-H framework (C=C-H). The presence of O-H group was confirmed by a broad hump centered around 3400 cm<sup>-1</sup>. In the <sup>13</sup>C CP-MAS NMR spectra (Figure S2), a strong peak appears at 129 ppm, which may be attributed to the presence of the phenyl ring carbon in the crosslinked framework. A hump at a slightly higher value (139 ppm) of the spectrum was recognized for the successful sulfonation of the phenyl ring in the polymer. The sulfonation of the precursor, THP, was also confirmed by analyzing the elemental contents of the polymer before and after the sulfonation step (Table S1). The thermal stability of the polymers was investigated using

thermogravimetric analysis (TGA) (Figure S3). Both THP and THP-SO<sub>3</sub>H possess high thermal stability at temperatures up to 700 °C. THP undergoes a minor weight loss of 2.3 % till 300 °C, beyond which thermal degradation of C–H and C–C bonds takes place leading to a decrease in the thermogram.<sup>6</sup> The thermal decomposition of the sulfonated polymer, THP-SO<sub>3</sub>H occurs at a lower temperature than its precursor polymer, which may be due to the desulfonation of acid groups at a temperature of around 200 °C.<sup>7</sup> Moreover, 4% weight loss can be observed up to 100 °C in the thermogram of THP-SO<sub>3</sub>H because of the evaporation of absorbed water molecules in the sulfonic acid sites. Nevertheless, retention of a high carbon mass percentage of THP-SO<sub>3</sub>H even at a high temperature of 700 °C suggests good thermal stability of the polymer. FESEM images of THP-SO<sub>3</sub>H reveal the presence of aggregated clusters of irregular particles (Figure S4). The FESEM images obtained are typically observed in organic polymers with a highly porous framework.<sup>8</sup> High surface area and accessible pores in a polymer are beneficial for the incorporation of sulfonic acid groups. The N<sub>2</sub> adsorption-desorption isotherms of THP polymer is shown in Figure S5. The N<sub>2</sub> isotherm displays a small knee at low relative pressure, which could be attributed to the presence of some micropores present.<sup>9</sup> However, the hysteresis loop in the type IV isotherm indicates towards the phenomena of capillary condensation occurring in the mesopores.<sup>10</sup> The BET surface area of the THP polymer, calculated from the multi-point BET method is 995 m<sup>2</sup>g<sup>-1</sup>. The porosity profile of THP was also investigated with the help of a pore-size distribution plot (Figure S6). The presence of both micropores and mesopores in the material provides a suitable platform for introducing accessible sulfonic acid sites.

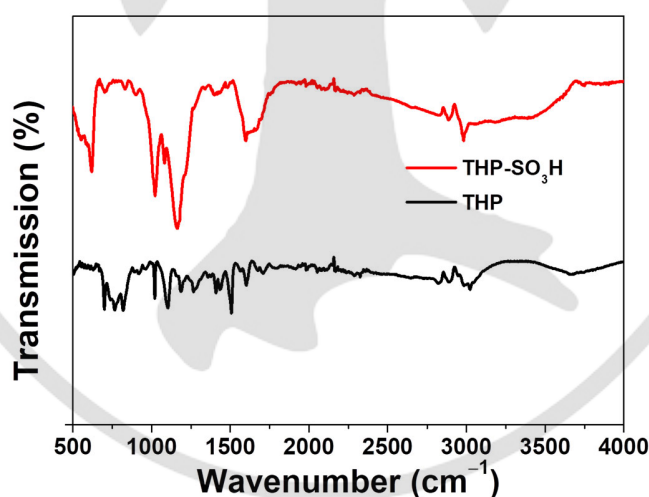


**Figure S1:** FT-IR spectrum of THP and THP-SO<sub>3</sub>H materials.

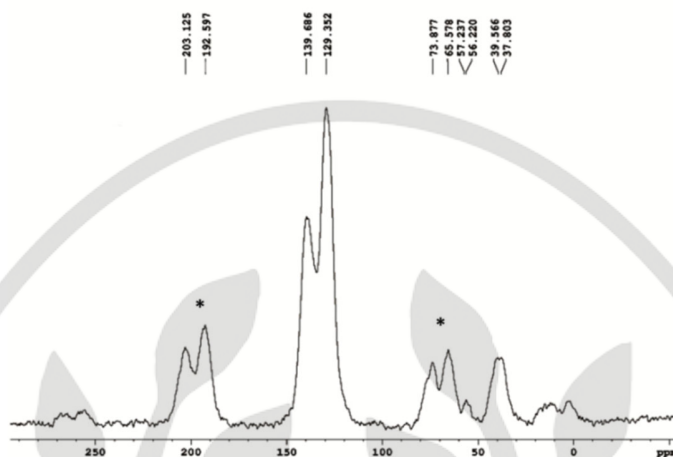


**Figure S2:**  $^{13}\text{C}$  CP-MAS NMR spectrum THP-SO<sub>3</sub>H material. Spinning side bands are denoted by asterisk (\*) symbols.

**Table S1:** Elemental content obtained from CHNS analysis

Sample	C (%)	H (%)	O (%)	S (%)
THP	73.9	4.4	21.7	-
THP-SO <sub>3</sub> H	63.0	4.7	23.8	8.5

Oxygen content was calculated by subtracting the total elemental content from 100%.

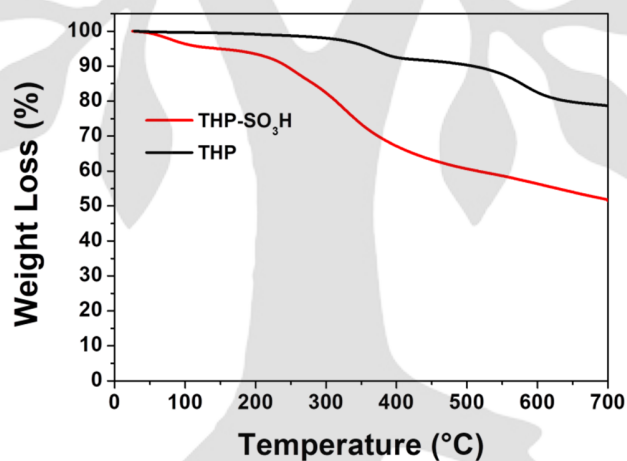


**Figure S3:** TGA plots of THP and THP-SO<sub>3</sub>H materials.

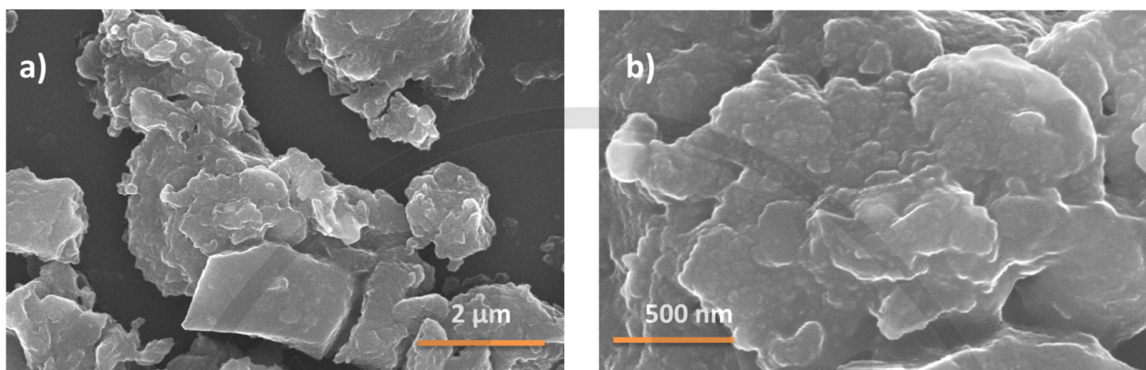


**Figure S4:** FESEM images of THP-SO<sub>3</sub>H material at a) 25000X and b) 150000X magnifications.

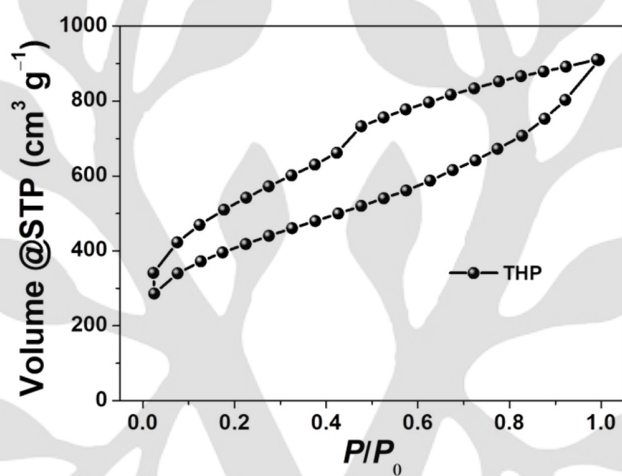


**Figure S5:** N<sub>2</sub> adsorption-desorption isotherm of the precursor, THP material.

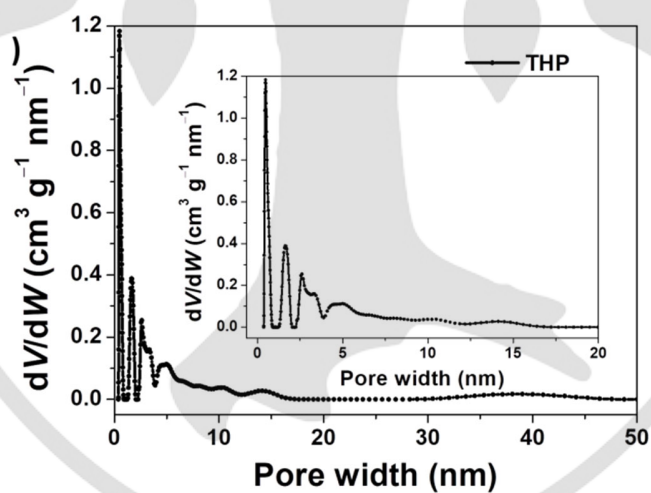


**Figure S6:** Pore-size distribution plot of the precursor, THP material.

#### 4. Calculation of acid strength of THP-SO<sub>3</sub>H material <sup>11</sup>

A 100 mL round-bottom flask equipped with a magnetic bar was charged with the sulfonated material THP-SO<sub>3</sub>H (100 mg) and 50 mL water. The flask was placed in constant temperature oil-bath at 40 °C. The mixture was stirred for 8 h at 40 °C. After 8 h, the mixture was cooled to room temperature. 10 mL aqueous mixture of THP-SO<sub>3</sub>H was taken in a 100 mL conical flask and 10 mL NaOH solution of strength 0.02894 (N) was added to it and allowed to stir for overnight. After filtration, the excess NaOH solution was back titrated with 0.112 (N) oxalic acid solution. 0.6 mL of oxalic acid solution was consumed to reach the first equivalence point of oxalic acid.

The amount of acid per 1 g of the THP-SO<sub>3</sub>H was calculated by the following method:

$$V_{(NaOH)} \times S_{(NaOH)} = V_{(OX)} \times S_{(OX)}$$

$$V_{(NaOH)} \times 0.02894 = 0.6 \times 0.112$$

$$V_{(NaOH)} = 2.322 \text{ mL}$$

So, the NaOH required to neutralize the acidic site of the THP-SO<sub>3</sub>H = (10-2.322) mL = 7.678 mL.

$$V_{(NaOH)} \times S_{(NaOH)} = V_{(THP-SO_3H)} \times S_{(THP-SO_3H)}$$

$$7.678 \times 0.02894 = 10 \times S_{(THP-SO_3H)}$$

$$S_{(THP-SO_3H)} = 0.02222 \text{ (N)}$$

The equivalent weight of -SO<sub>3</sub>H group = 81.

#### Calculation:

1000 mL 1 (N) THP-SO<sub>3</sub>H = 81 g free -SO<sub>3</sub>H group in the sulfonated material (THP-SO<sub>3</sub>H)

Therefore, 50 mL 0.02222 (N) THP-SO<sub>3</sub>H = 0.089991 g free -SO<sub>3</sub>H group  
= 1.111 mmol free -SO<sub>3</sub>H group

So, 50 mL 0.02222 (N) THP-SO<sub>3</sub>H aqueous mixture contains 0.089991 g free -SO<sub>3</sub>H site

i.e. 100 mg of THP-SO<sub>3</sub>H sample contains 1.111 mmol free -SO<sub>3</sub>H site

Therefore, 1000 mg of THP-SO<sub>3</sub>H sample contains 11.11 mmol free -SO<sub>3</sub>H site.

#### 5. General procedure for the optimization of reaction conditions

A 25 mL round-bottom flask equipped with a magnetic bar and water condenser were charged with substrates **1a** (480 mg, 1.0 mmol), **2a** (246 mg, 3.0 mmol), solvent (2.0 mL) and THP-SO<sub>3</sub>H (96 mg) in air atmosphere. The flask was placed in a constant temperature oil-bath at 80 °C, and the progress of the reaction was monitored by TLC. After the specified time as mentioned in Table 1 of the manuscript, the solvent was removed under reduced pressure and the crude product was purified by dry column vacuum chromatography (silica gel G, petroleum ether 60-80 °C/EtOAc).

## 6. General procedure for the synthesis of TRAMs 3a-g

A 25 mL round-bottom flask equipped with a magnetic bar and water condenser were charged with **1** (1.0 mmol), **2a** (3.0 mmol), DCE (2.0 mL) and THP-SO<sub>3</sub>H (96 mg) in an air atmosphere. The flask was placed in a constant temperature oil-bath at 80 °C and the progress of the reaction was monitored by TLC. After the specified time as mentioned in Scheme 1 of the manuscript, the mixture was filtered to separate the catalyst and washed twice with DCE (2 x 5 mL). Then the filtrate was removed under reduced pressure and the crude product was purified by dry column vacuum chromatography (silica gel G, petroleum ether 60-80 °C/EtOAc) to obtain the desired product.

## 7. General procedure for the synthesis of TRAMs 3h-q and 4

A 25 mL round-bottom flask equipped with a magnetic bar and water condenser were charged with **1** (1.0 mmol), **2** (2.0 mmol), DCE (2.0 mL) and THP-SO<sub>3</sub>H (96 mg) in an air atmosphere. The flask was placed in a constant temperature oil-bath at 80 °C and the progress of the reaction was monitored by TLC. After the specified time as mentioned in Scheme 1 of the manuscript, the mixture was filtered to separate the catalyst and washed twice with DCE (2 x 5 mL). Then the filtrate was removed under reduced pressure and the crude product was purified by dry column vacuum chromatography (silica gel G, petroleum ether 60-80 °C/EtOAc) to obtain the desired product.

## 8. General procedure for recyclability of the catalyst THP-SO<sub>3</sub>H

A 25 mL round-bottom flask equipped with a magnetic bar and water condenser were charged with **1a** (1.0 mmol), **2a** (3.0 mmol), DCE (2.0 mL) and TMOP-SO<sub>3</sub>H (96 mg) in an air atmosphere. The flask was placed in a constant temperature oil-bath at 80 °C and the progress of the reaction was monitored by TLC. After 30 min, the catalyst was recovered by simple filtration, washed twice with DCE and dried at 100 °C under vacuum oven for 3 h. Then the recovered catalyst was used for further four cycles. The crude product was purified after each cycle to get the isolated yield.

## 9. FT-IR spectra of THP-SO<sub>3</sub>H material after the fifth cycle.

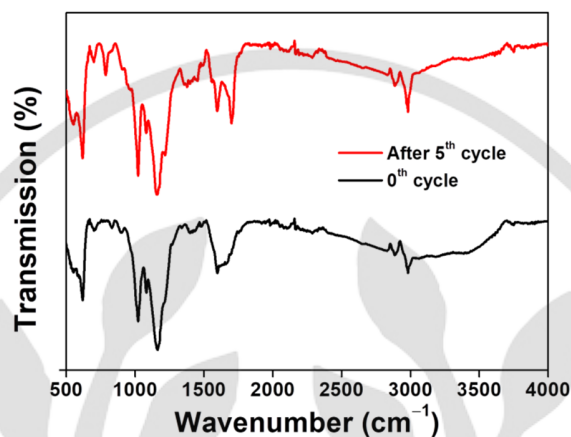
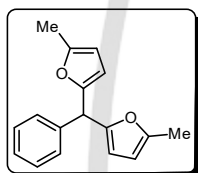
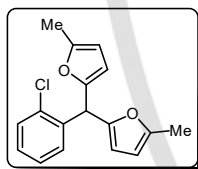


Figure S7: FT-IR spectra of THP-SO<sub>3</sub>H material after the fifth cycle.

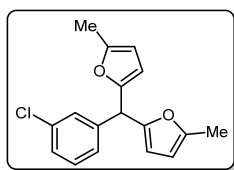
## 10. Analytical data of products 3 and 4



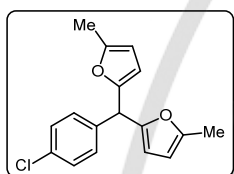
5,5'-(Phenylmethylene)bis(2-methylfuran) (**3a**):<sup>3</sup> Yellow oily liquid. <sup>1</sup>H NMR (400 MHz, CDCl<sub>3</sub>):  $\delta$  (ppm) 2.158 (s, 6H), 5.256 (s, 1H), 5.788 (d,  $J = 3.2$  Hz, 4H), 7.159–7.243 (m, 5H). <sup>13</sup>C NMR (100 MHz, CDCl<sub>3</sub>):  $\delta$  (ppm) 13.65, 45.12, 106.08, 108.19, 126.97, 128.40, 128.44, 140.00, 151.46, 152.85.



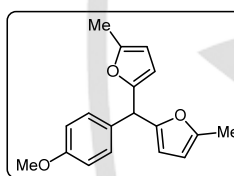
5,5'-((2-Chlorophenyl)methylene)bis(2-methylfuran) (**3b**):<sup>12</sup> Yellow oily liquid. <sup>1</sup>H NMR (400 MHz, CDCl<sub>3</sub>):  $\delta$  (ppm) 2.240 (s, 6H), 5.297 (s, 1H), 5.883 (s, 4H), 7.114–7.140 (m, 1H), 7.215–7.236 (m, 3H). <sup>13</sup>C NMR (100 MHz, CDCl<sub>3</sub>):  $\delta$  (ppm) 13.61, 44.75, 106.16, 108.46, 126.63, 127.20, 128.54, 129.66, 134.23, 142.05, 151.71, 151.96.



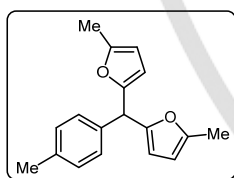
5,5'-((3-Chlorophenyl)methylene)bis(2-methylfuran) (**3c**):<sup>12</sup> Yellow oily liquid. <sup>1</sup>H NMR (400 MHz, CDCl<sub>3</sub>):  $\delta$  (ppm) 2.234 (s, 6H), 5.840–5.878 (m, 5H), 7.172–7.186 (m, 3H), 7.346–7.371 (m, 1H). <sup>13</sup>C NMR (100 MHz, CDCl<sub>3</sub>):  $\delta$  (ppm) 13.64, 41.62, 106.11, 108.75, 126.85, 128.26, 129.60, 129.94, 133.82, 137.46, 151.56, 151.66.



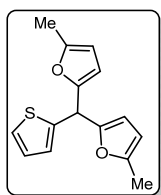
5,5'-((4-Chlorophenyl)methylene)bis(2-methylfuran) (**3d**):<sup>3</sup> Yellow liquid. <sup>1</sup>H NMR (400 MHz, CDCl<sub>3</sub>):  $\delta$  (ppm) 2.162 (s, 6H), 5.222 (s, 1H), 5.780–5.809 (m, 4H), 7.097 (d,  $J = 8.4$  Hz, 2H), 7.195 (d,  $J = 8.4$  Hz, 2H). <sup>13</sup>C NMR (100 MHz, CDCl<sub>3</sub>):  $\delta$  (ppm) 12.54, 43.43, 105.05, 107.27, 127.52, 128.70, 131.71, 137.50, 150.59, 151.18.



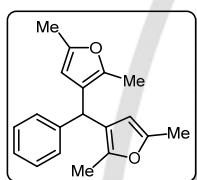
5,5'-((4-Methoxyphenyl)methylene)bis(2-methylfuran) (**3e**):<sup>12</sup> Yellow liquid. <sup>1</sup>H NMR (400 MHz, CDCl<sub>3</sub>):  $\delta$  (ppm) 2.168 (s, 6H), 3.714 (s, 3H), 5.208 (s, 1H), 5.761–5.803 (m, 4H), 6.773 (d,  $J = 8.8$  Hz, 2H), 7.092 (d,  $J = 8.4$  Hz, 2H). <sup>13</sup>C NMR (100 MHz, CDCl<sub>3</sub>):  $\delta$  (ppm) 13.63, 44.30, 55.24, 106.01, 107.97, 113.80, 129.36, 132.15, 151.36, 153.17, 158.53.



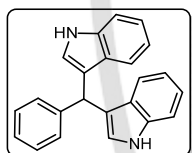
5,5'-(*p*-Tolylmethylene)bis(2-methylfuran) (**3f**):<sup>3</sup> Yellow liquid. <sup>1</sup>H NMR (400 MHz, CDCl<sub>3</sub>):  $\delta$  (ppm) 2.159 (s, 6H), 2.246 (s, 3H), 5.218 (s, 1H), 5.770–5.5.788 (m, 4H), 7.024–7.076 (s, 4H). <sup>13</sup>C NMR (100 MHz, CDCl<sub>3</sub>):  $\delta$  (ppm) 12.57, 20.03, 43.71, 104.98, 106.97, 127.19, 128.08, 135.46, 136.00, 150.30, 152.02.



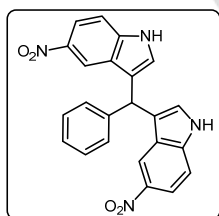
5,5'-(Thiophen-2-ylmethylene)bis(2-methylfuran) (**3g**):<sup>3</sup> Yellow liquid. <sup>1</sup>H NMR (400 MHz, CDCl<sub>3</sub>): δ (ppm) 2.274 (s, 6H), 5.603 (s, 1H), 5.904–5.913 (m, 2H), 5.995 (d, *J* = 2.8 Hz, 2H), 6.891–6.904 (m, 1H), 6.937–6.959 (m, 1H), 7.213 (dd, *J* = 5.2 Hz and 1.2 Hz, 1H). <sup>13</sup>C NMR (100 MHz, CDCl<sub>3</sub>): δ (ppm) 13.63, 40.15, 106.17, 107.88, 124.52, 125.61, 126.56, 143.22, 151.55, 152.16.



3,3'-(Phenylmethylene)bis(2,5-dimethylfuran) (**3h**):<sup>3</sup> Yellow oil. <sup>1</sup>H NMR (400 MHz, CDCl<sub>3</sub>): δ (ppm) 2.056 (s, 6H), 2.123 (s, 6H), 4.851 (s, 1H), 5.651 (s, 2H), 7.102–7.209 (m, 5H). <sup>13</sup>C NMR (100 MHz, CDCl<sub>3</sub>): δ (ppm) 11.69, 13.60, 37.92, 107.33, 121.93, 126.04, 128.10, 128.20, 143.96, 145.41, 149.22.

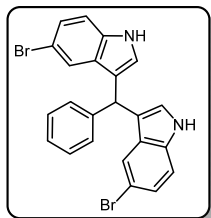


3,3'-(Phenylmethylene)bis(1*H*-indole) (**3i**):<sup>3</sup> White solid. <sup>1</sup>H NMR (400 MHz, CDCl<sub>3</sub>): δ (ppm) 5.798 (s, 1H), 6.509 (d, *J* = 2.4 Hz, 2H), 6.924 (d, *J* = 7.6 Hz, 2H), 7.066–7.319 (m, 11H), 7.715 (s, 2H). <sup>13</sup>C NMR (100 MHz, CDCl<sub>3</sub>): δ (ppm) 40.19, 111.07, 119.23, 119.67, 119.95, 121.93, 123.66, 126.16, 127.07, 128.25, 128.75, 136.66, 144.02.

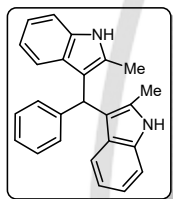


3,3'-(Phenylmethylene)bis(5-nitro-1*H*-indole) (**3j**):<sup>3</sup> Yellowish solid. <sup>1</sup>H NMR (600 MHz, DMSO-*d*<sub>6</sub>): δ (ppm) 6.066 (s, 1H), 6.998 (s, 1H), 7.085–7.268 (m, 5H), 7.402 (d, *J* = 8.8 Hz, 2H), 7.832

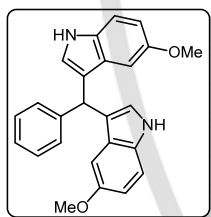
(d,  $J = 8.0$  Hz, 2H), 8.179 (s, 2H), 11.544 (br, 2H).  $^{13}\text{C}$  NMR (150 MHz, DMSO- $d_6$ ):  $\delta$  (ppm) 54.98, 112.19, 116.28, 116.70, 120.59, 125.83, 126.46, 127.66, 128.26, 128.53, 139.85, 140.23, 143.82.



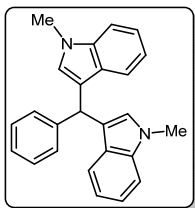
3,3'-(Phenylmethylene)bis(5-bromo-1*H*-indole) (**3k**):<sup>3</sup> Yellowish solid.  $^1\text{H}$  NMR (400 MHz,  $\text{CDCl}_3$ ):  $\delta$  (ppm) 5.758 (s, 1H), 6.652–6.657 (m, 2H), 7.250 (d,  $J = 0.8$  Hz, 3H), 7.271 (s, 2H), 7.296–7.311 (m, 4H), 7.477 (s, 2H), 8.131 (s, 2H).



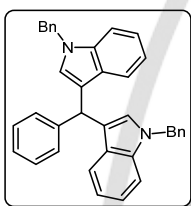
3,3'-(Phenylmethylene)bis(2-methyl-1*H*-indole) (**3l**):<sup>3</sup> White solid.  $^1\text{H}$  NMR (400 MHz,  $\text{CDCl}_3$ ):  $\delta$  (ppm) 1.985 (s, 6H), 5.936 (s, 1H), 6.782 (t,  $J = 7.6$  Hz, 2H), 6.898–6.983 (m, 4H), 7.153–7.223 (m, 7H), 7.642–7.676 (m, 2H).  $^{13}\text{C}$  NMR (100 MHz,  $\text{CDCl}_3$ ):  $\delta$  (ppm) 29.71, 39.23, 109.94, 113.39, 119.04, 119.32, 120.58, 125.95, 128.09, 129.07, 130.95, 131.80, 135.02, 143.72.



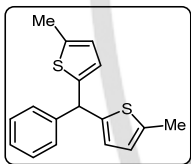
3,3'-(Phenylmethylene)bis(5-methoxy-1*H*-indole) (**3m**):<sup>3</sup> Yellowish solid.  $^1\text{H}$  NMR (400 MHz,  $\text{CDCl}_3$ ):  $\delta$  (ppm) 3.626 (s, 6H), 5.711 (s, 1H), 6.601–6.609 (m, 2H), 6.732–6.777 (m, 4H), 7.169–7.238 (m, 5H), 7.274–7.299 (m, 2H), 7.791–7.804 (m, 2H).  $^{13}\text{C}$  NMR (100 MHz,  $\text{CDCl}_3$ ):  $\delta$  (ppm) 40.28, 55.60, 101.92, 111.68, 111.87, 119.26, 124.45, 126.43, 127.92, 128.67, 128.72, 131.85, 143.93, 153.66.



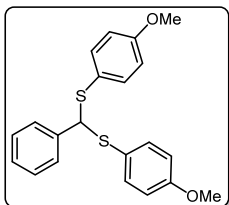
3,3'-(Phenylmethylene)bis(1-methyl-1*H*-indole) (**3n**):<sup>3</sup> White solid. <sup>1</sup>H NMR (400 MHz, CDCl<sub>3</sub>): δ (ppm) 3.573 (s, 6H), 5.807 (s, 1H), 6.446 (s, 2H), 6.894–6.993 (m, 2H), 7.096–7.140 (m, 3H), 7.175–7.213 (m, 4H), 7.261–7.318 (m, 4H). <sup>13</sup>C NMR (100 MHz, CDCl<sub>3</sub>): δ (ppm) 32.71, 40.14, 109.12, 118.29, 118.69, 120.09, 121.47, 126.08, 127.50, 128.25, 128.32, 128.74, 137.45, 144.51.



3,3'-(Phenylmethylene)bis(1-benzyl-1*H*-indole) (**3o**):<sup>3</sup> White solid. <sup>1</sup>H NMR (400 MHz, CDCl<sub>3</sub>): δ (ppm) 5.174 (s, 4H), 5.916 (s, 1H), 6.635 (s, 2H), 6.936–7.008 (m, 6H), 7.069–7.110 (m, 2H), 7.168–7.272 (m, 11H), 7.347–7.402 (m, 4H). <sup>13</sup>C NMR (100 MHz, CDCl<sub>3</sub>): δ (ppm) 39.81, 49.46, 109.27, 118.35, 118.49, 119.75, 121.22, 125.67, 125.98, 129.93, 127.33, 127.49, 127.81, 128.21, 128.30, 136.57, 137.43, 143.65.

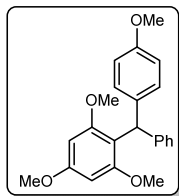


5,5'-(Phenylmethylene)bis(2-methylthiophene) (**3p**):<sup>13</sup> Yellow oil. <sup>1</sup>H NMR (400 MHz, CDCl<sub>3</sub>): δ (ppm) 2.411 (s, 6H), 5.672 (s, 1H), 6.566–6.590 (m, 4H), 7.219–7.313 (m, 5H). <sup>13</sup>C NMR (100 MHz, CDCl<sub>3</sub>): δ (ppm) 14.88, 47.27, 124.03, 125.19, 126.49, 127.82, 127.95, 138.59, 143.31, 144.75.

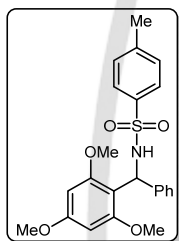


(Phenylmethylene)bis((4-methoxyphenyl)sulfane) (**3q**):<sup>3</sup> Yellow liquid. <sup>1</sup>H NMR (400 MHz, CDCl<sub>3</sub>): δ (ppm) 3.741 (s, 6H), 5.159 (s, 1H), 6.755 (d, *J* = 8.8 Hz, 4H), 7.209–7.285 (m, 9H). <sup>13</sup>C

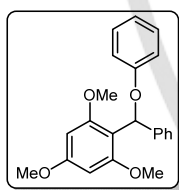
NMR (100 MHz, CDCl<sub>3</sub>):  $\delta$  (ppm) 55.31, 62.99, 114.36, 124.81, 127.83, 127.92, 128.33, 135.96, 140.16, 159.96.



1,3,5-Trimethoxy-2-((4-methoxyphenyl)(phenyl)methyl)benzene (**4a**):<sup>3</sup> Pale yellow oil. <sup>1</sup>H NMR (400 MHz, CDCl<sub>3</sub>):  $\delta$  (ppm) 3.587 (s, 6H), 3.775 (s, 3H), 3.798 (s, 3H), 5.998 (s, 1H), 6.143 (s, 2H), 6.779 (d,  $J$  = 8.8 Hz, 2H), 7.108–7.170 (m, 5H), 7.191–7.228 (m, 2H). <sup>13</sup>C NMR (100 MHz, CDCl<sub>3</sub>):  $\delta$  (ppm) 43.78, 54.69, 54.75, 55.23, 91.11, 112.46, 124.67, 126.98, 128.38, 129.68, 135.54, 144.13, 156.88, 158.55, 159.41.



4-Methyl-*N*-(phenyl(2,4,6-trimethoxyphenyl)methyl)benzenesulfonamide (**4b**):<sup>2</sup> White solid. <sup>1</sup>H NMR (400 MHz, CDCl<sub>3</sub>):  $\delta$  (ppm) 2.198 (s, 3H), 3.515 (s, 6H), 3.638 (s, 3H), 5.778 (s, 2H), 6.005 (d,  $J$  = 10.8 Hz, 1H), 6.147 (d,  $J$  = 10.8 Hz, 1H), 6.901 (d,  $J$  = 8.0 Hz, 2H), 7.094–7.161 (m, 5H), 7.402 (d,  $J$  = 8.0 Hz, 2H). <sup>13</sup>C NMR (100 MHz, CDCl<sub>3</sub>):  $\delta$  (ppm) 21.37, 51.49, 55.31, 55.59, 90.54, 108.73, 126.43, 126.58, 126.84, 127.91, 128.66, 137.54, 141.29, 142.39, 157.89, 160.86.



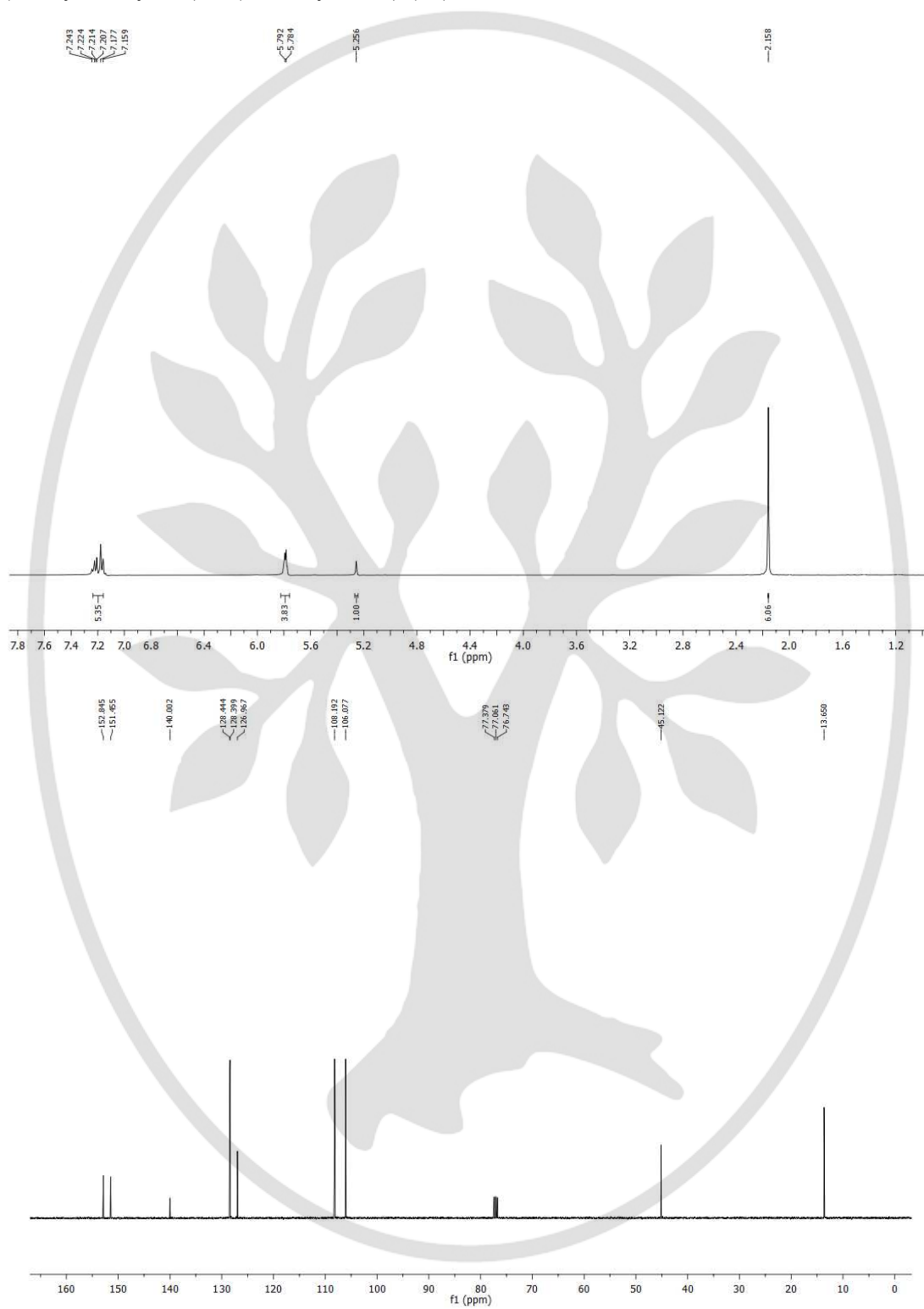
1,3,5-Trimethoxy-2-(phenoxy(phenyl)methyl)benzene (**4c**): Yellow liquid. <sup>1</sup>H NMR (400 MHz, CDCl<sub>3</sub>):  $\delta$  (ppm) 3.584 (s, 6H), 3.798 (s, 3H), 5.979 (s, 1H), 6.143 (s, 2H), 6.69 (d,  $J$  = 8.8 Hz, 2H), 7.063–7.256 (m, 8H). <sup>13</sup>C NMR (100 MHz, CDCl<sub>3</sub>):  $\delta$  (ppm) 44.48, 55.44, 55.90, 91.83, 113.99, 114.59, 125.39, 127.68, 129.08, 130.53, 136.41, 144.71, 153.45, 159.23, 160.10. Anal. Calcd. (%) for C<sub>22</sub>H<sub>22</sub>O<sub>4</sub>: C 75.41, H 6.33; Found: C 75.46, H 6.29.

## 11. References

- (1) Zeng, J. H.; Wang, Y. F.; Gou, S. Q.; Zhang, L. P.; Chen, Y.; Jiang, J. X.; Shi, F. *ACS Appl. Mater. Interfaces* **2017**, *9*, 34783.
- (2) Paul, D.; Borah, A.; Khatua, S.; Chatterjee P. N. *Asian J. Org. Chem.* **2019**, *8*, 1870.
- (3) Paul, D.; Khatua, S.; Chatterjee, P. N. *ChemistrySelect* **2018**, *3*, 11649.
- (4) Rao, C. N. R.; Venkataraghavan, R.; Kasturi, T. R. *Can. J. Chem.* **1964**, *42*, 36.
- (5) Suganuma, S.; Nakajima, K.; Kitano, M.; Hayashi, S.; Hara, M. *ChemSusChem* **2012**, *5*, 1841.
- (6) Kundu, S. K.; Singuru, R.; Hayashi, T.; Hijikata, Y.; Irle, S.; Mondal, J. *ChemistrySelect* **2017**, *2*, 4705.
- (7) Du, M.; Agrawal, A. M.; Chakraborty, S.; Garibay, S. J.; Limvorapitux, R.; Choi, B.; Madrahimov, S. T.; Nguyen, S. T. *ACS Sustain. Chem. Eng.* **2019**, *7*, 8126.
- (8) (a) Deka, N.; Patidar, R.; Kasthuri, S.; Venkatramaiah, N.; Dutta, G. K. *Mater. Chem. Front.* **2019**, *3*, 680. (b) Nath, I.; Chakraborty, J.; Heynderickx, P. M.; Verpoort, F. *Appl. Catal. B: Environmental* **2018**, *227*, 102.
- (9) Silvestre-Albero, J.; Silvestre-Albero, A.; Rodríguez-Reinoso, F.; Thommes, M. *Carbon* **2012**, *50*, 3128.
- (10) Ravishankar, T. N.; Ramakrishnappa, T.; Nagaraju, G.; Rajanaika, H. *ChemistryOpen* **2015**, *4*, 146.
- (11) Bhunia, S.; Banerjee, B.; Bhaumik, A. *Chem. Commun.* **2015**, *51*, 5020.
- (12) Thirupathi, P.; Soo Kim, S. *J. Org. Chem.* **2010**, *75*, 5240.
- (13) Dhiman, S.; Ramasastry, S. *Org. Biomol. Chem.* **2013**, *11*, 8030.

## 12. $^1\text{H}$ and $^{13}\text{C}$ NMR spectra of products 3 and 4

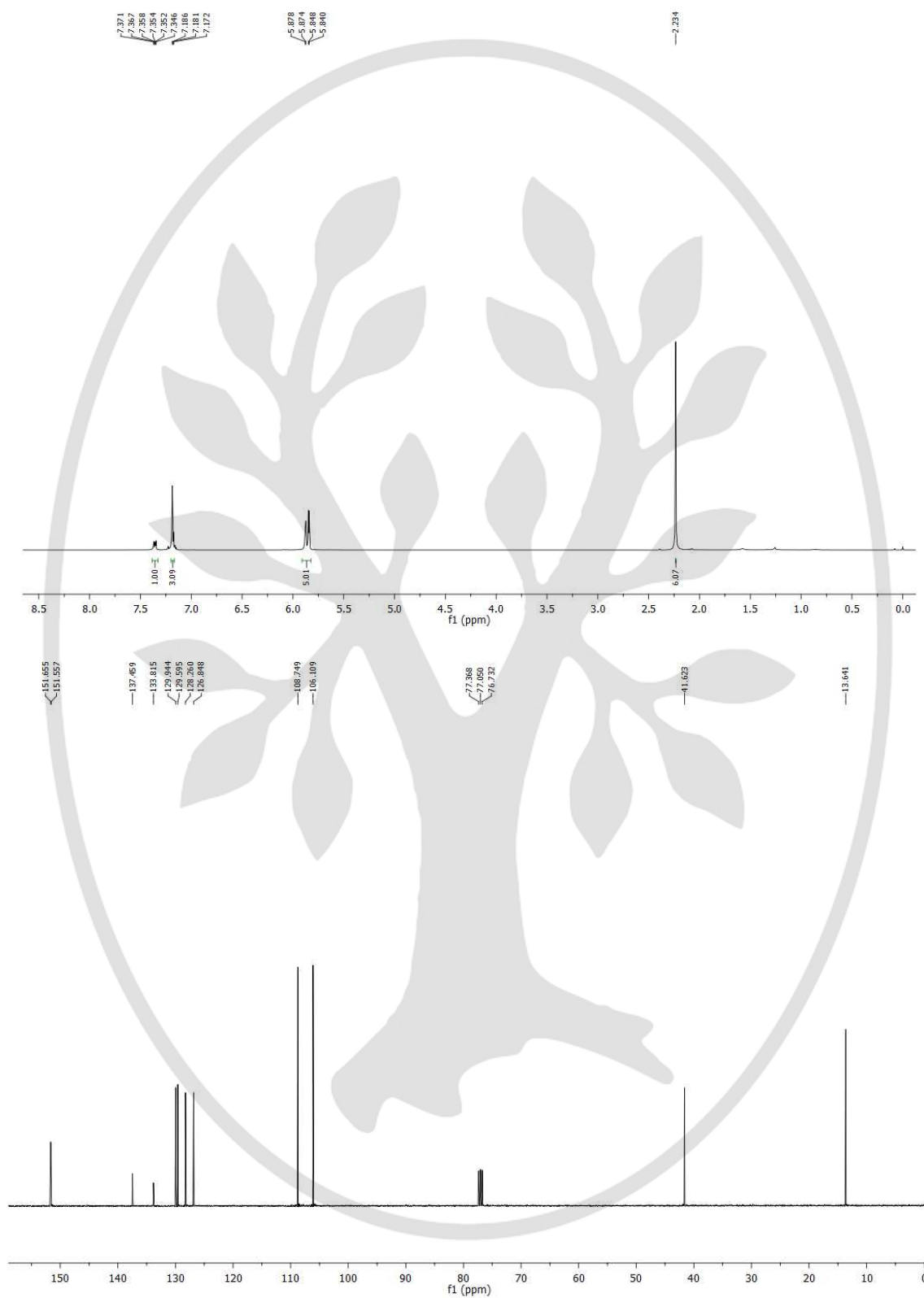
### 5,5'-(Phenylmethylene)bis(2-methylfuran) (**3a**)



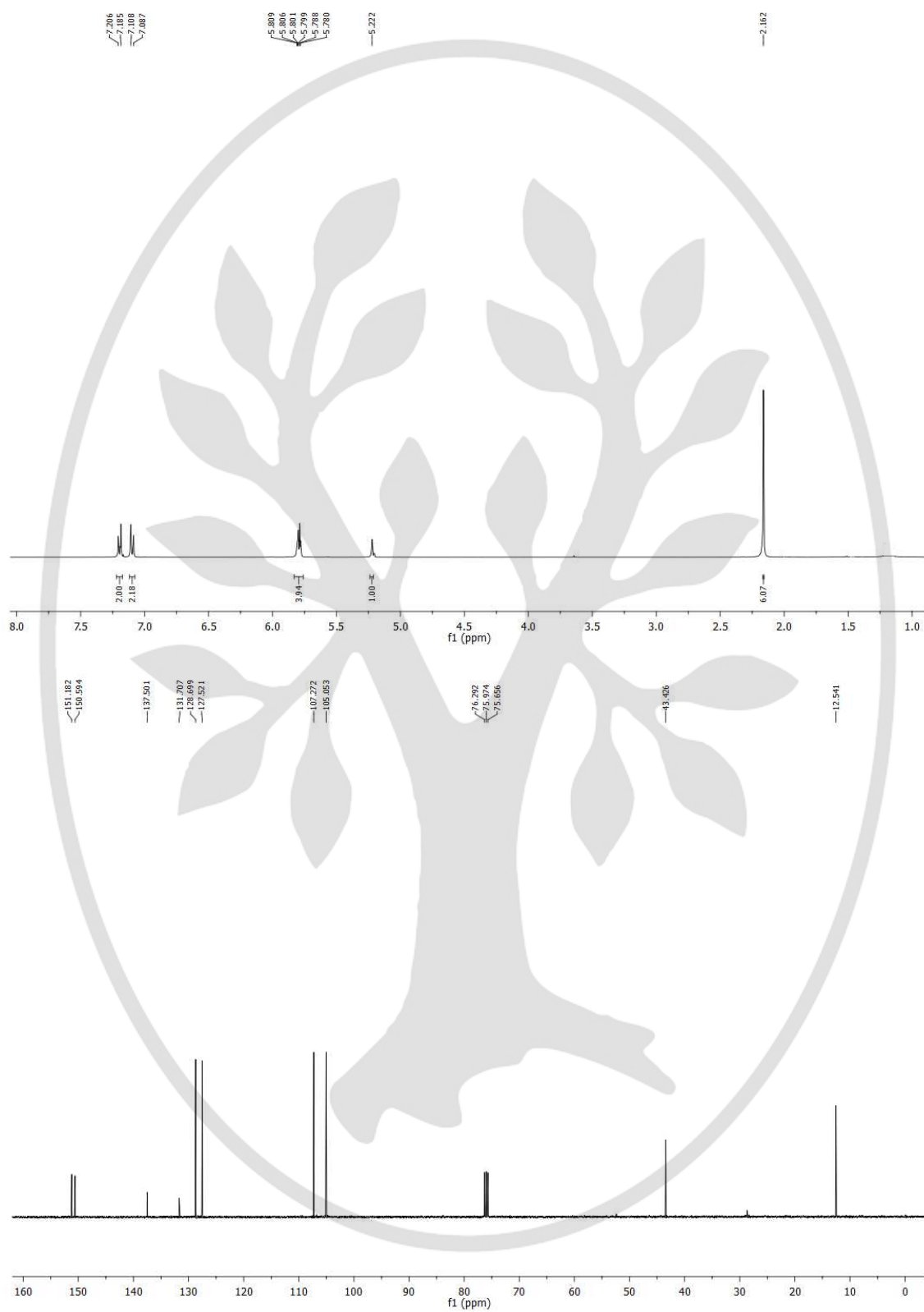
5,5'-((2-Chlorophenyl)methylene)bis(2-methylfuran) (**3b**)



5,5'-((3-Chlorophenyl)methylene)bis(2-methylfuran) (**3c**)



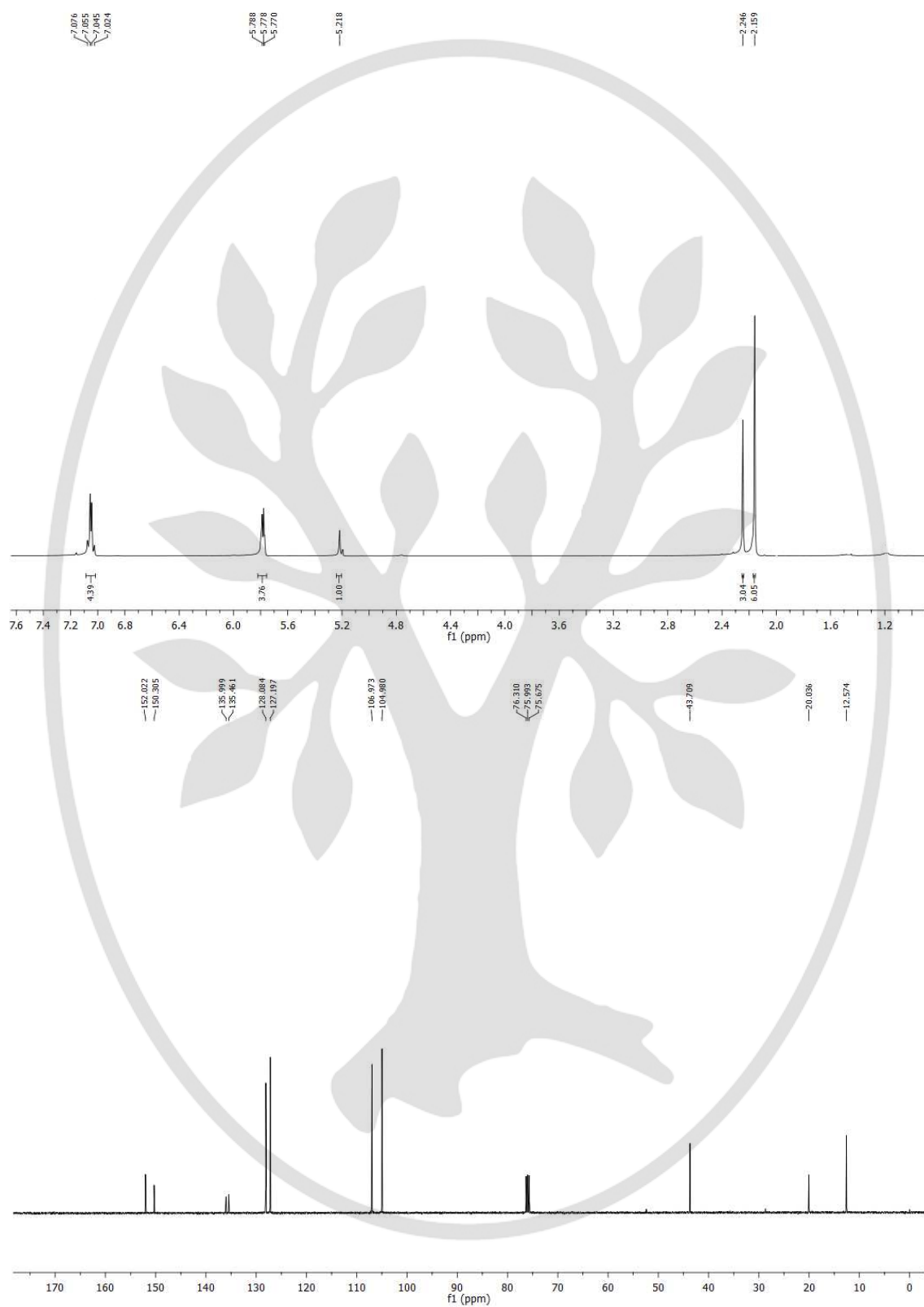
5,5'-((4-Chlorophenyl)methylene)bis(2-methylfuran) (**3d**)



5,5'-((4-Methoxyphenyl)methylene)bis(2-methylfuran) (**3e**)



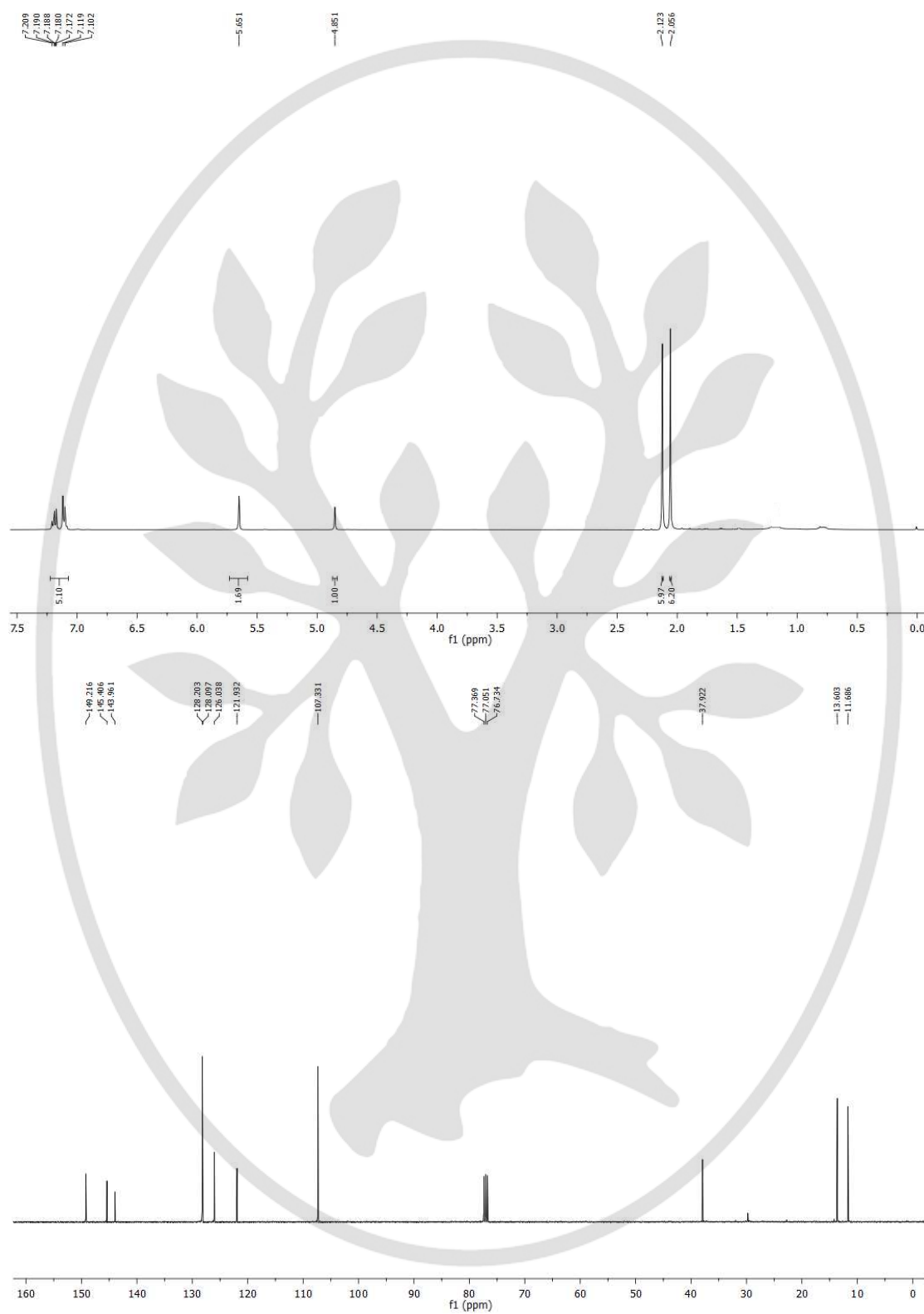
5,5'-(*p*-Tolylmethylene)bis(2-methylfuran) (**3f**)



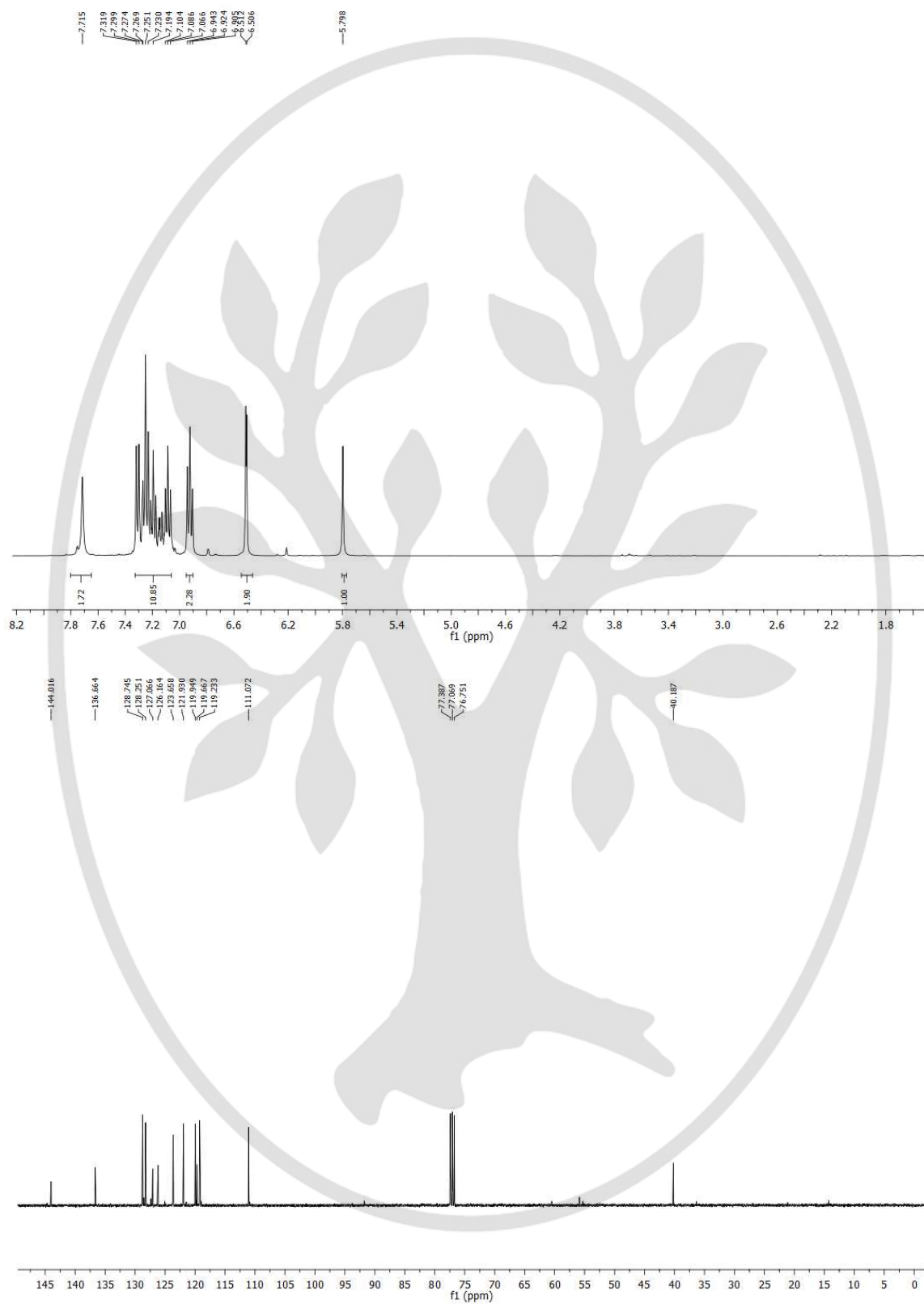
5,5'-(Thiophen-2-ylmethylene)bis(2-methylfuran) (**3g**)



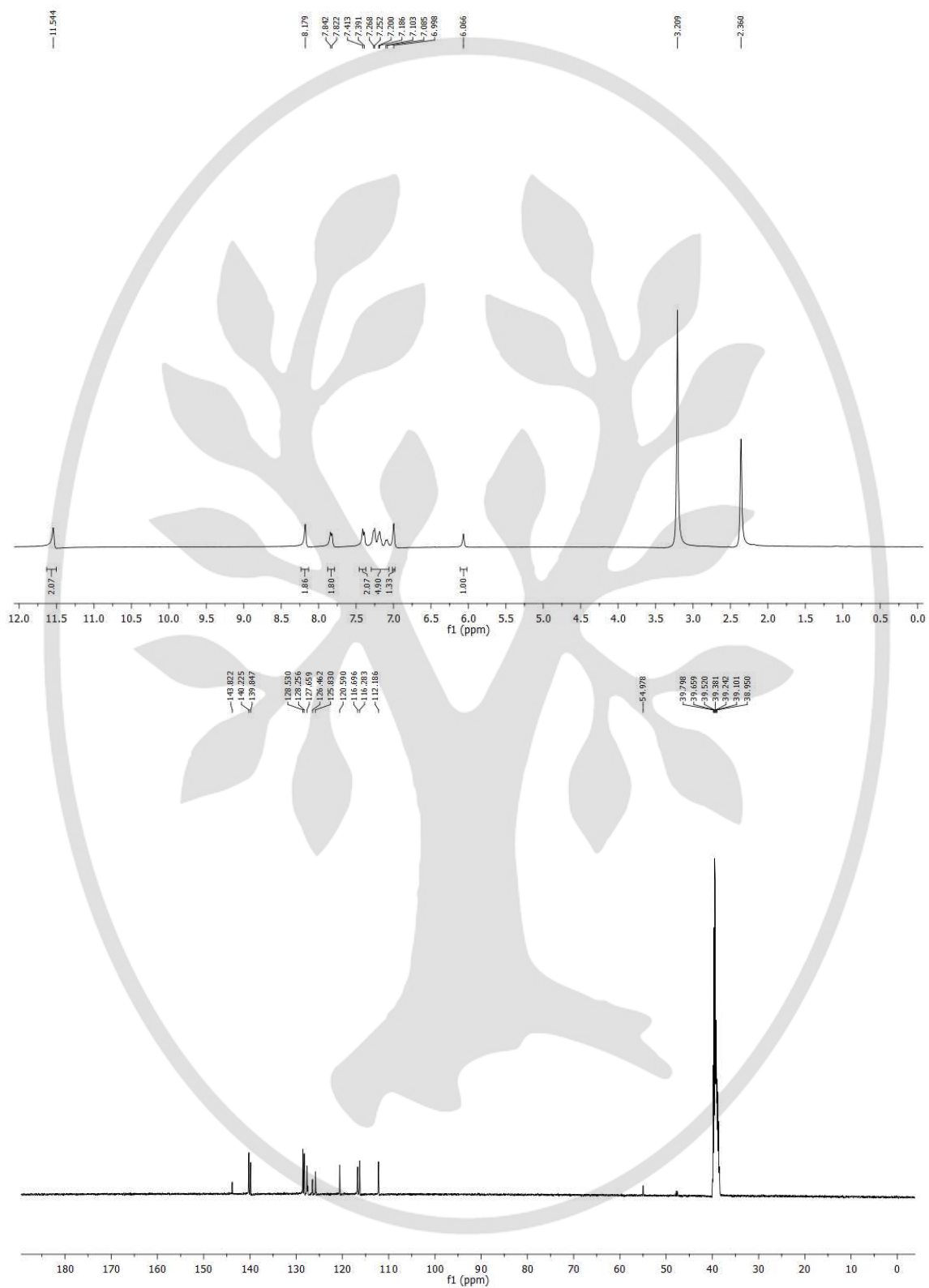
3,3'-(Phenylmethylene)bis(2,5-dimethylfuran) (**3h**)



3,3'-(Phenylmethylene)bis(1*H*-indole) (**3i**)



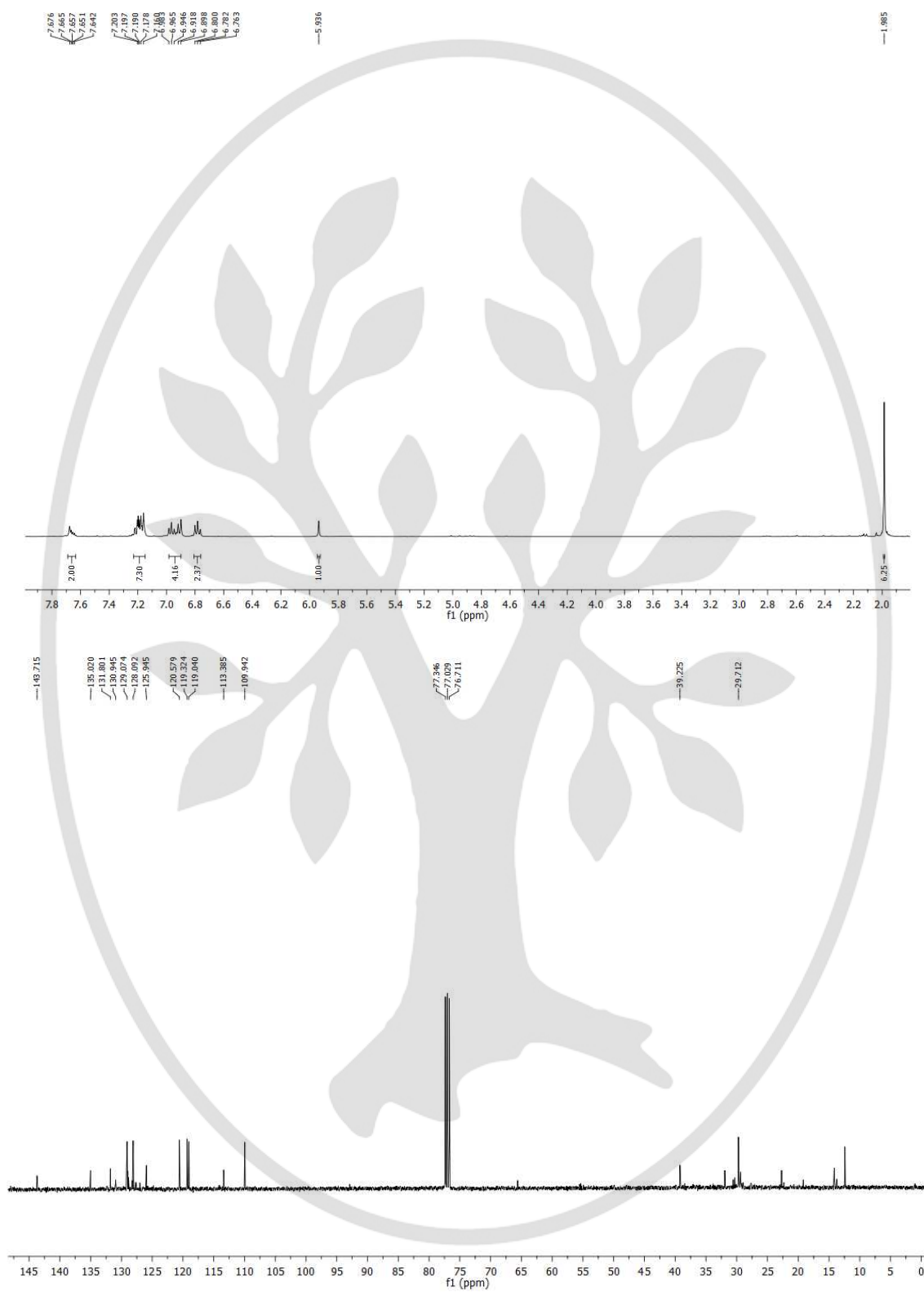
3,3'-(Phenylmethylene)bis(5-nitro-1H-indole) (**3j**)



3,3'-(Phenylmethylene)bis(5-bromo-1*H*-indole) (**3k**)



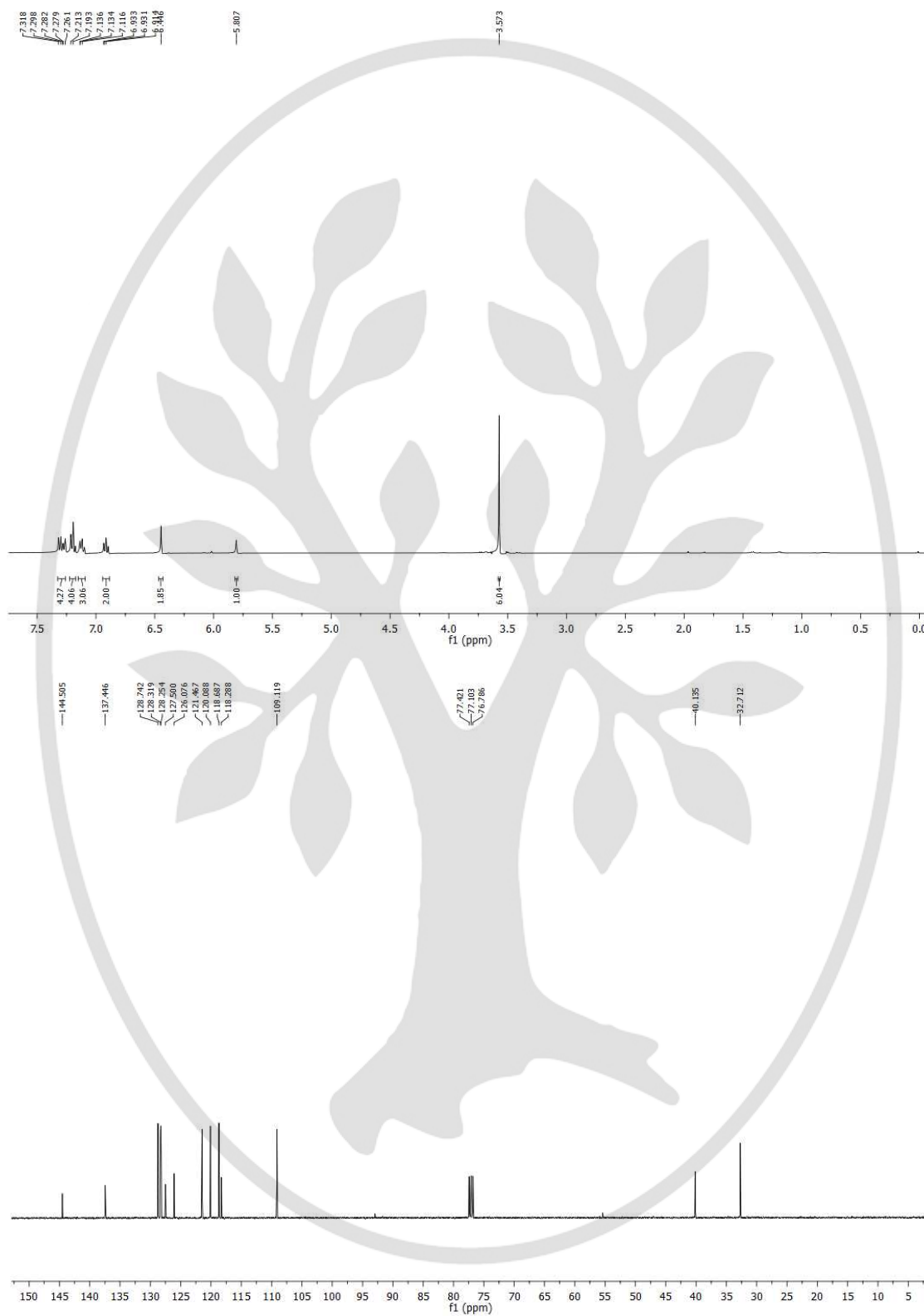
3,3'-(Phenylmethylene)bis(2-methyl-1H-indole) (**31**)



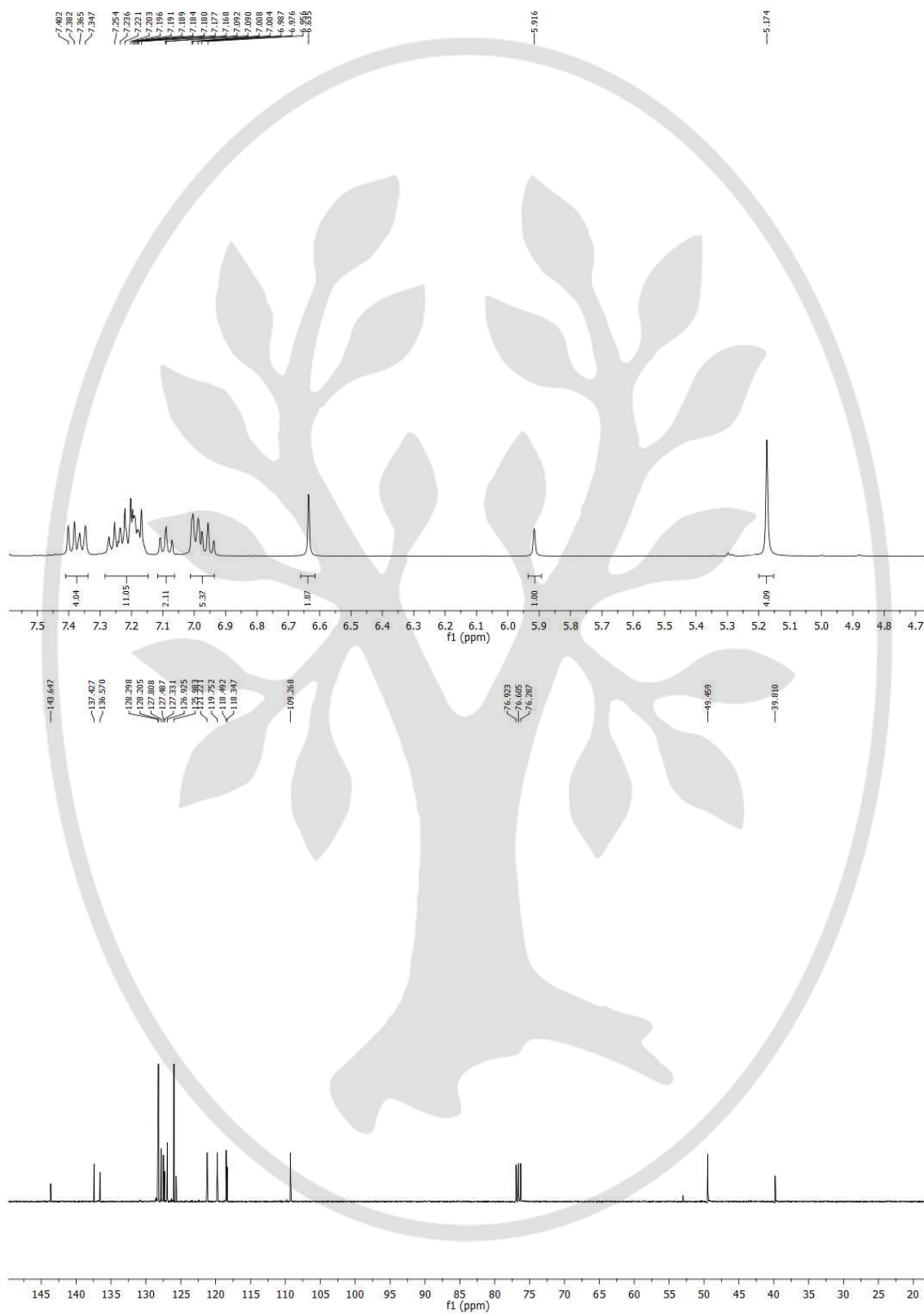
3,3'-(Phenylmethylene)bis(5-methoxy-1H-indole) (**3m**)



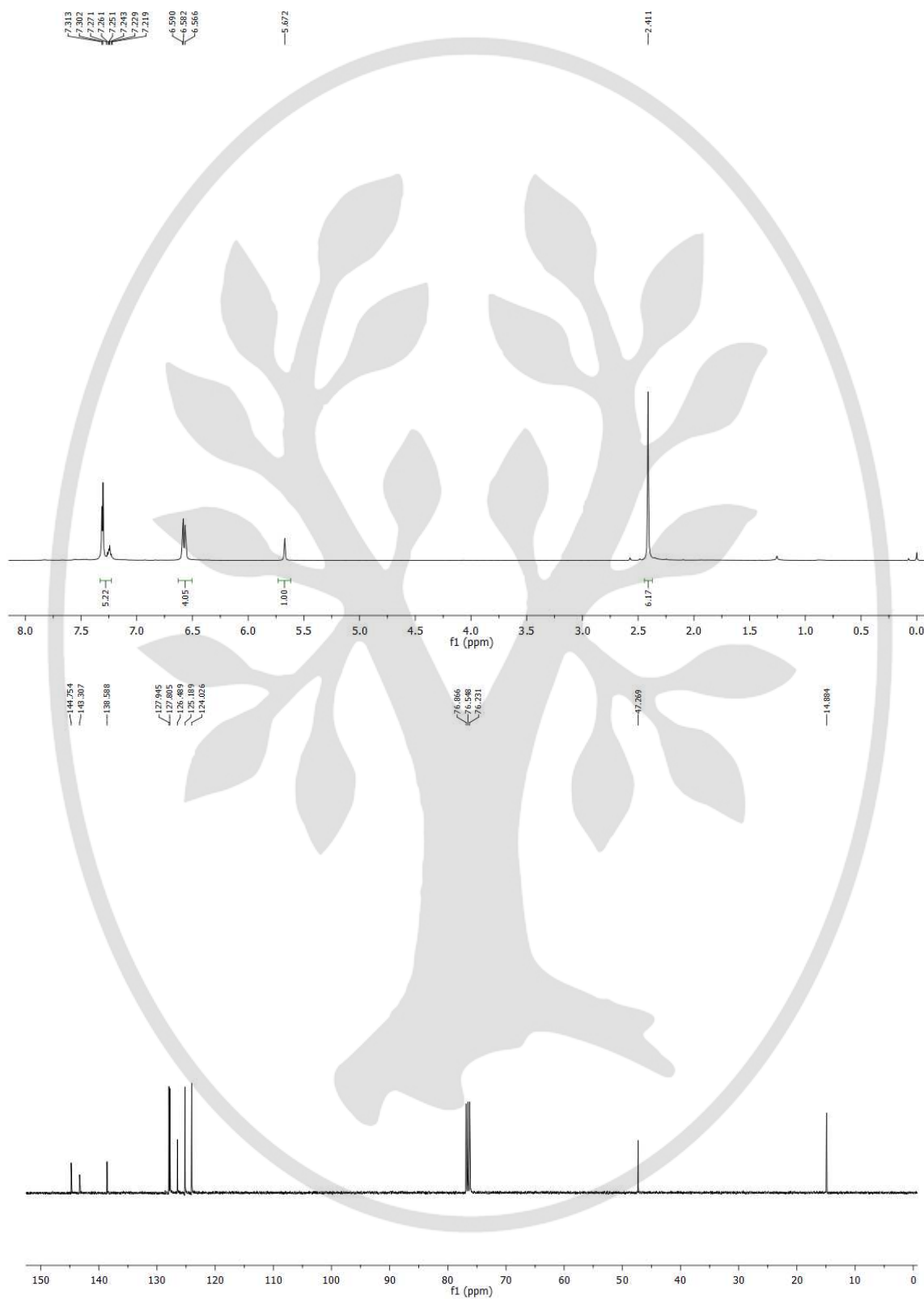
3,3'-(Phenylmethylene)bis(1-methyl-1*H*-indole) (**3n**)



3,3'-(Phenylmethylene)bis(1-benzyl-1*H*-indole) (**30**)



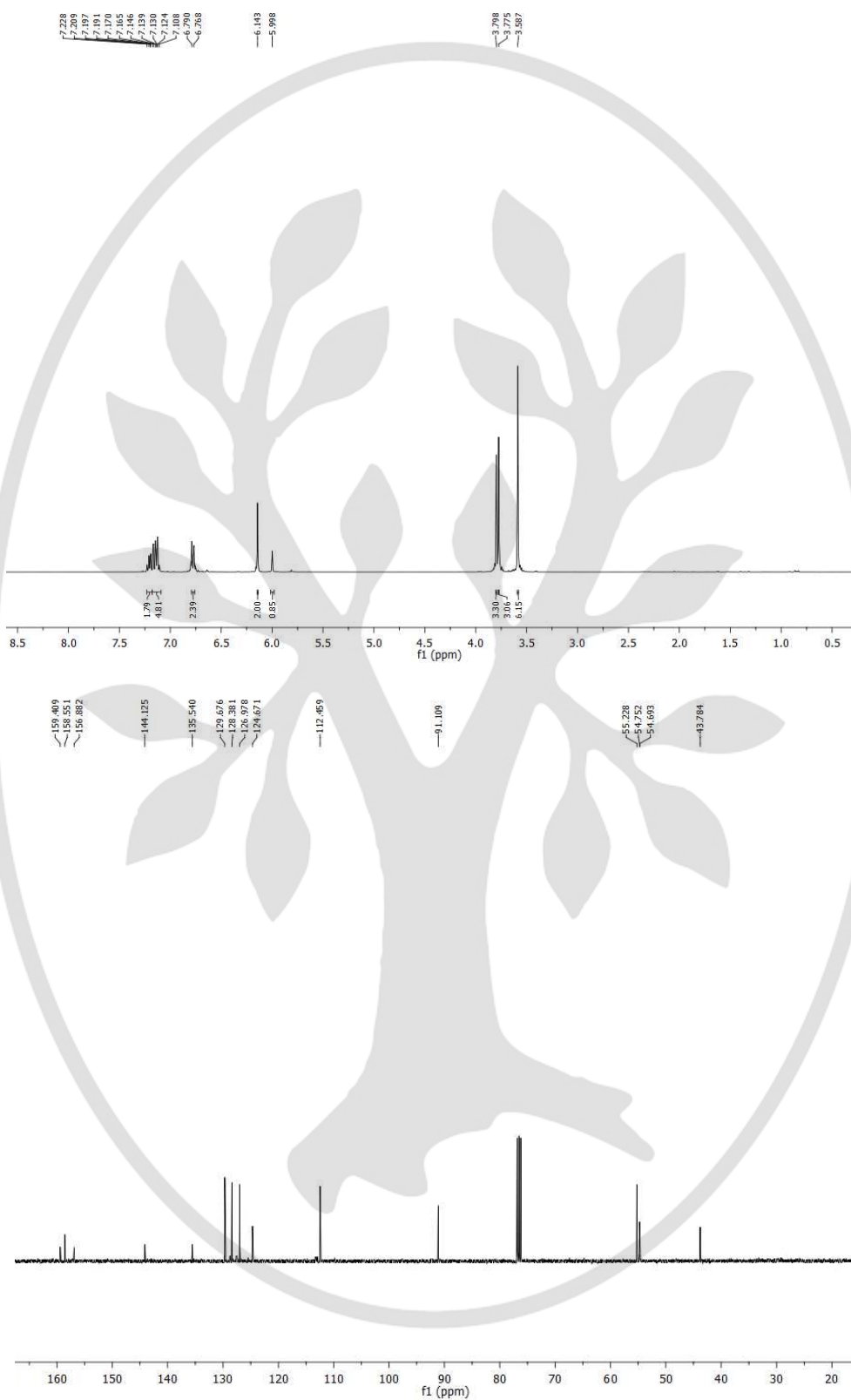
5,5'-(Phenylmethylene)bis(2-methylthiophene) (**3p**)



(Phenylmethylene)bis((4-methoxyphenyl)sulfane) (**3q**)



1,3,5-Trimethoxy-2-((4-methoxyphenyl)(phenyl)methyl)benzene (**4a**)



4-Methyl-*N*-(phenyl(2,4,6-trimethoxyphenyl)methyl)benzenesulfonamide (**4b**)



1,3,5-Trimethoxy-2-(phenoxy(phenyl)methyl)benzene (4c)

